DURBAN UNIVERSITY OF TECHNOLOGY

Application of optimal control for power systems considering renewable energy technologies

By

Dhanpal Chetty

Student Number: 19100522

A dissertation submitted in fulfilment of the requirements for the degree of Master of Engineering in Electrical Power Engineering

In the Department of Electrical Power Engineering
Faculty of Engineering and Built Environment

Supervisor: Dr. G. Sharma

Co-Supervisor: Prof. I.E. Davidson

March 2021

DECLARATION

This dissertation is the student's own work, every cited work or text have been appropriately referenced. It has not been partially or fully submitted at any other University.

This research was duly supervised by Dr. G. Sharma and Prof. I.E. Davidson, at the Durban University of Technology.

Submitted by:

…… ……

Dhanpal Chetty Date

Student Number: 19100522

Approved for Final Submission by:

…… ……

Supervisor: Dr. G. Sharma Date

…… ……

Co-Supervisor: Prof I. E. Davidson Date

PUBLICATION ARISING

Dhanpal Chetty

Faculty of Engineering and Built Environment

Master of Engineering in Electrical Power Engineering

Journal Paper

D Chetty, G Sharma and I Davidson, “Active Power Regulation of the Power System considering DFIG based Wind Power in coordination with TCPS-SMES”, International Energy Journal, vol. 19, pp. 189–198, 2019.

DEDICATION

For

Ama & Dada

ACKNOWLEDGMENTS

My beautiful, wife and children, your enduring love and support makes me want to do better and be better.

Dr. Gulshan Sharma, you have my most sincere appreciation for your calm and professional demeanor, your patience and all the assistance you provided me, without which, I would not have been able to complete this research.

Prof. Innocent Davidson, I thank you for your support through this challenging journey.

Dr. Evans Ojo, I am sincerely grateful for the guidance you provided me, in writing this thesis.

Mr. Milan Joshi, Mr. Anuoluwapo Aluko and Dr. Buraimoh Elutunji, my fellow postgraduate students at DUT, thank you for all your assistance during these past two years.

My colleagues in the Department of Electrical Power Engineering, thank you for all your support and friendship over the many years.

(Nelson)

ABSTRACT

Over the last decade, power generation from renewable energy sources such as wind, hydro and solar energies have substantially increased globally and in South Africa. Of all the renewable energy sources, wind energy appears to be the most promising, considering design and costs. However, due to the intermittent nature of wind, the increased integration of wind energy into existing power systems raises several control challenges related to load frequency control (LFC) and tie-line power system stability. The stability of modern power systems, incorporating wind energy generations, will be significantly enhanced with the development of LFC strategies based on modern control theory, which is the focus of this research.

This thesis presents the design, modelling and analysis, of two LFC control strategies for interconnected power systems, having wind power integrations. The first design is an optimal control strategy, based on error minimization through full state vector feedback, for a two-area interconnected power system consisting of hydro-thermal generations. The second design is a model predictive control (MPC) strategy, based output vector feedback of system state parameters, for a two-area interconnected power system consisting of thermal generations in each area. Both designs include the active power support from doubly fed induction generator based wind turbines (DFIG) in conjunction with the combined effort of a thyristor control phase shifter (TCPS) and super conducting magnetic energy storage unit (SMES). Both control strategies were simulated in MATLAB Simulink and positive results were obtained. The results show that the optimal control strategy is enhanced with power integrations using DFIG based wind turbines combined with the TCPS-SMES units and the MPC strategy is very robust and provides better dynamic performances even with parameter variations and generation rate restrictions.

TABLE OF CONTENTS

DECLARATION……..i

DEDICATION ii

ACKNOWLEDGEMENT iii

ABSTRACT iv

LIST of FIGURES ix

LIST of TABLES xi

LIST of ACRONYMS xii

LIST of SYMBOLS……xiv

CHAPTER ONE: INTRODUCTION 1

1.1 Context of the Research 1

1.2 Motivation for the Research 4

1.3 Problem Statement ..... ……..4

1.4 Aim and Objectives 5

1.4.1 Aims of this Research 5

1.4.2 Objectives for the Optimal Control Strategy 6

1.4.3 Objectives for the MPC Strategy 6

1.5 Research Outputs 7

1.6 Dissertation Structure 7

CHAPTER TWO: LITERATURE REVIEW 9

2.1 Renewable Energy Penetration 9

2.2 Hydropower Generation 9

2.3 Wind Power Generation 10

2.4 Synchronous Generators 13

2.5 Induction Generators 15

2.6 Doubly Fed Induction Generators 17
2.7 FACTS Devices 21
2.8 Load Frequency Control Strategies 27
2.9 Conclusion 28
CHAPTER THREE: OPTIMAL CONTROL STRATEGDY 30
3.1 Introduction 30
3.2 Review of Optimal Control Strategies 30
3.3 Models under Study 33
3.4 Modelling of a Wind Generation System incorporating DFIG 36
3.5 Modelling of TCPS 37
3.6 Modelling of a SMES Unit 40
3.7 Modelling of the Optimal Controller 43
3.8 System Vector for the Optimal Control Design 44
3.9 Simulation Results and Analysis 45
3.10 Discussion 54
3.11 Conclusion 55
CHAPTER FOUR: MODEL PREDICTIVE CONTROL 56
4.1 Introduction 56
4.2 Review of the Model Predictive Control Strategy 56
4.3 Model under Study 58
4.4 Generation Rate Constraints Model 58
4.5 Model Predictive Control Design 60
4.6 Simulations Results and Discussion 61
4.7 Conclusion 68
CHAPTER FIVE: CONCLUSION 69
CONCLUSION 69

SCOPE FOR FUTURE RESEARCH 69

REFERENCES 79

Appendix A: Hydro-Thermal Power Plant Data 83
Appendix B: Data for DFIG Based Wind Turbines……..83
Appendix C: Thermal-Thermal Power Plant Data……..…84
Appendix D: Optimal Control System Matrices……...85

LIST OF FIGURES

Figure Number	Figure Caption	Page Number
1.1:	Total additional new capacity build until 2030	1
1.2:	Location of the REDZs overlaid onto the electricity grid infrastructure corridors	3
1.3:	Cost per energy unit of different energy sources	3
2.1:	Illustrative power system	11
2.2:	Power in a conventional power plant	12
2.3:	WECS using a multipole synchronous generator	14
2.4:	Grid connect SCIG [21]	16
2.5:	Variable resistance induction generator	16
2.6:	Grid connected DFIG	17
3.1:	Two area interconnected system with hydro-thermal generation.	33
3.2:	Two area hydro-thermal interconnected power system incorporating DFIG based wind turbines	34
3.3:	Two area hydro-thermal interconnected power system incorporating DFIG in conjunction with TCPS-SMES.	35
3.4:	The transfer function of DFIG based wind turbine	36
3.5:	Model of a two-area interconnected power system with TCPS in series with tie-line	37
3.6:	Transfer function of the TCPS	40
3.7:	Schematic diagram of SMES unit	40
3.8:	Transfer function of the SMES unit	42
3.9a:	Frequency response in area one	50
3.9b:	Frequency response in area two	50
3.9c:	Tie-line power response	51

3.9d: Area control error for 1% load alteration in the hydro power plant 51

3.10a: Frequency response in area one 52

3.10b: Frequency response in area two 52

3.10c: Tie-line power response 53

3.10d: Area control response 53

4.1: The Transfer function model of a two-area interconnected power system with DFIG in coordination control of TCPS-SMES 59

4.2: Non-linear turbine model with GRC 59

4.3: Simplified schematic diagram of MPC scheme 61

4.4a: Frequency response in area one for 1 % load increase in area 62

4.4b: Frequency response in area two for 1 % load increase in area 62

4.4c: Tie-line power response for 1 % load fluctuation in area one 63

4.4d: Area control error for 1 % load fluctuation in area one 63

4.5a: Frequency response in area one for 1 % load increase in area one 64

4.5b: Frequency response in area two for 1 % load in area one 64

4.5c: Tie-line power response for 1 % load fluctuation in area one 65

4.5d: Area control error for 1 % load fluctuation in area one 65

4.6a: Frequency response in area one with 1% load increase in area one and 25 % variation in system parameters 66

4.6b: Frequency response in area two with1% load increase in area one and 25 % variation in system parameters 66

4.6c: Tie-line power response for 1% load increase in area one and 25 % variation in system parameters. 67

4.6d: Area control error for 1% load increase in area one and 25 % variation in system parameters. 68

LIST OF TABLES

Table Number	Table Caption	Page Number
1.1:	Generated capacity in South Africa	4
3.1:	Optimum PI values for the three developed models	46
3.2:	Feedback gains for each state of the three developed models	48
3.3:	Eigenvalues analysis for the three developed models	49

LIST OF ACRONYMS

AC	Alternating current
ACE	Area control error
BESS	Battery energy storage system
DC	Direct current
DFIG	Doubly fed induction generator
REDZS	Renewable Energy Development Zones
EIC	“Essence of emulation”
FSWT	Fixed-speed wind turbine
FACTS	Flexible Alternating Current Transmission System
GRC	Generation rate constraints
GSC	Grid side convertor
HVDC	High voltage direct current
IRP	Integrated Resource Plan
LQR	Linear quadratic regulator
LFC	Load frequency control
LTC	Load Tap Changes
MPPT	Maximum power tracking
MPC	Model predictive control
OSID	OptiSlip induction generator
PMSG	Permanent magnet synchronous generator
RBF	Redox flow battery
REIPPPP	Renewable Energy Independent Power Producer Procurement Programme
RSC	Rotor side convertor
SA	South African
SCIG	Squirrel-caged induction generator
SSSC	Static synchronous series compensator

List of acronyms continued

SMES	Super conducting magnetic energy storage
TCPS	Thyristor controlled phase shifters
VSWT	Variable-speed wind turbine
WECS	Wind energy conversion system
WRIG	Wound-rotor induction generator
WRSG	Wound-rotor synchronous generator

LIST OF SYMBOLS

ACE_i	Area control error
B_i	Frequency bias constant
K_{pi}	Power system gain
H_{ei}	Wind turbine inertia of area *i*
P_{ri}	*Rated area power output*
T_{pi}	Power system time constant (sec)
T_{ti}	Non reheat turbine time constant (sec)
ΔF_i	Incremental change in frequency
ΔP_{tie12}	Incremental change in tie-line power
ΔP_{hi}	Incremental change in governor valve position
ΔP_{di}	Incremental change in load demand for DFIG
$K_{\omega pi}$	DFIG proportional controller gain of area *i*
$K_{\omega ii}$	DFIG integral controller gain of area *i*
P_{mech}	Wind turbine mechanical output
T_{ai}	DFIG turbine time constant of area *i*
T_{wi}	Washout filter time constant for DFIG area *i*
ω_i	Wind turbine speed of area *i*
$\omega_{i\ max}$	Wind turbine cut-out speed maximum of area *i*
$\omega_{i\ min}$	Wind turbine cut-out speed minimum of area *i*
ω_{mech}	Angular velocity of rotor rotation
$\omega_{m,\ meas}$	Wind turbine measured mechanical speed
ΔP^*_f	Incremental wind turbine power set point
ΔP_{NCi}	Incremental DFIG active power output of area *i*
$\Delta P_{NCi,ref}$	Incremental wind turbine active power reference of
ΔP^*_ω	Incremental wind turbine power set point
$\Delta\ \omega_i$	Incremental wind turbine speed of area *i*

CHAPTER 1: INTRODUCTION

1.1 Context of the Research

South Africa currently faces an electricity crisis. This is mainly due to an aging electrical infrastructure combined with a situation where the load demand exceeds the generation capacity [1]. This resulted in Eskom, the state owned utility enterprise, implementing country wide load shedding measures. Load shedding reduces the load demand, by switching off parts of the distribution network in a planned and controlled manner, to maintain system stability and prevent power system shutdown. This significantly impacts on the industrial and commercial industries, thereby adversely affecting the economy of the country.

In 2011, the South African (SA) government adopted the Integrated Resource Plan (IRP) [2], which was revised in 2016, 2018 and 2019. This is a proposed development plan for building new power generation plants to meet the growing demand for the period 2010 to 2030. Figure (1.1) indicates that the plan includes 17,8 GW of renewables, with renewables accounting for 42 % of the proposed new power systems.

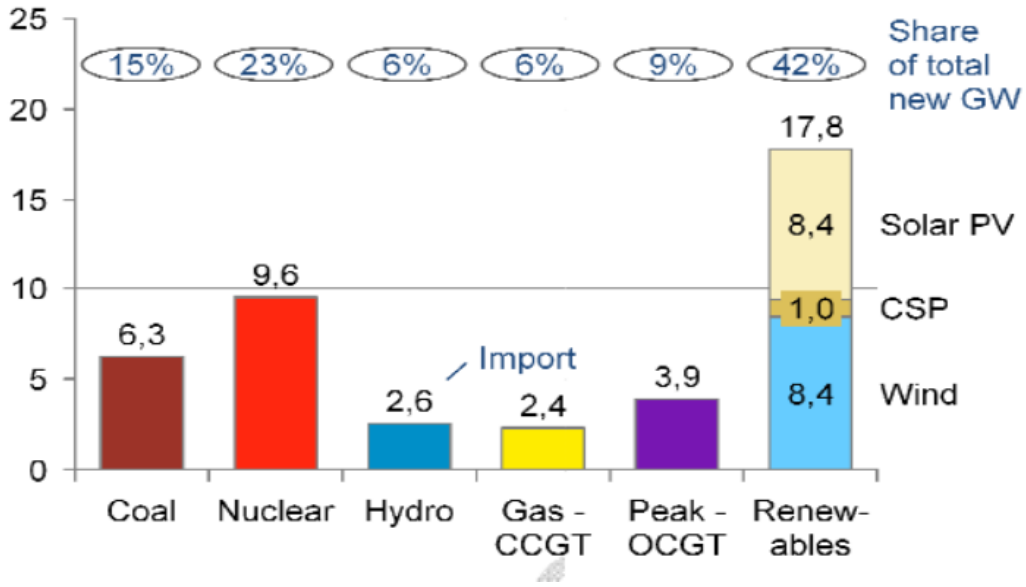

Figure 1.1: Total additional new capacity build until 2030 [2]

Energy security is essential for South Africa to develop and prosper economically. It is clearly evident from the legal and developmental policies adopted in [2–4]. SA is committed to a low carbon future, while trying to meet future load demands. These policies demonstrate a commitment to renewable energy and laid the foundation to SA's negotiations and ratification of the Paris Climate Agreement and becoming a signatory of United Nation's 2030 Agenda for Sustainable Development [5]. The success of these ambitious plans depends primarily on the momentum in advancing renewable energy for access to affordable, reliable and sustainable energy, for all its people. From the Renewable Energy Global Status Report for 2018 [6], it is clear that the world now adds more renewable power capacity annually, than it adds new capacity from fossil fuels. In 2017, renewable energy accounted for approximately 70 % of new power generation additions to the global power generating capacity.

However, SA still remains largely dependent on coal due to the abundance of supply and relatively low cost, although significant progress is being made in solar and wind energy penetration. According to stats SA [7], in 2013 the contribution of solar energy to the national grid was negligible, but climbed to 2151 GWh in 2016. Wind generation only contributed 18 GWh to the national grid in 2013, but climbed to 2126 GWh in 2016. In order to keep abreast of its renewable goals, the SA government created the Renewable Energy Independent Power Producer Procurement Programme (REIPPPP) [8], with the aim of securing electrical energy from the private sector via renewable energy sources, to add to the national grid. The program resulted in significant cost reductions for solar and wind generation over a relatively short period of time. In addition, in 2016 the government approved eight Renewable Energy Development Zones (REDZs) and five 'Power Corridors' [9]. In 2019 three additional REDZs were proposed for wind and solar generation expansion [10]. These REDZs and Power Corridors, publicised in figure (1.2), are geographical locations where wind and solar generations are being incentivized, with investment in the transmission infrastructure.

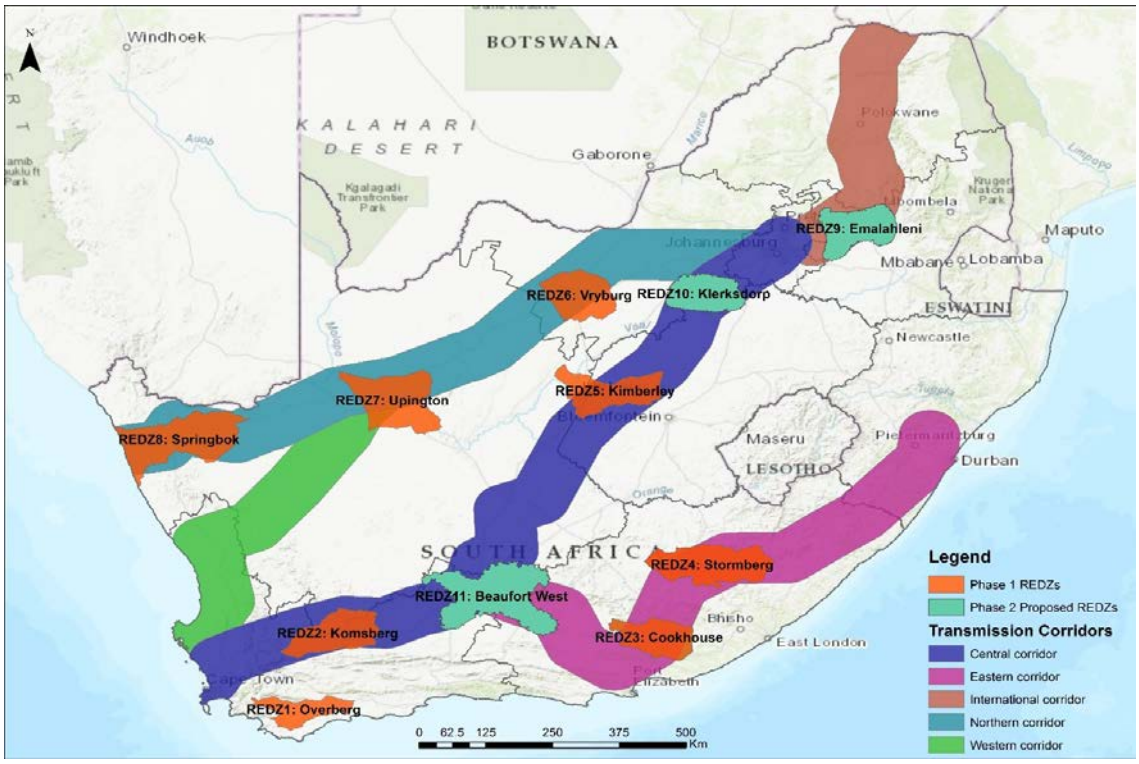

Figure 1.2: Location of the REDZs overlaid onto the electricity grid infrastructure corridors where investment in transmission infrastructure is planned [10].

Figure (1.3) points towards wind energy as the most promising, due to the relatively low generation costs compared to other renewable technologies [11].

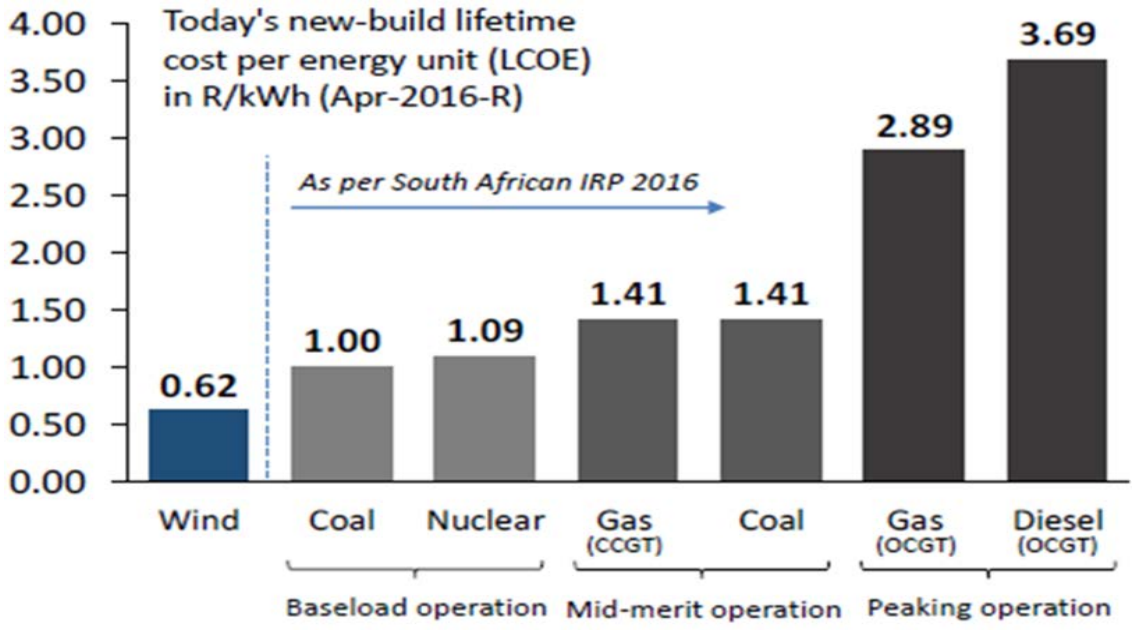

Figure 1.3: Cost per energy unit of different energy sources [11]

1.2 Motivation for the Research

Table (1.1) indicates that currently, in SA, coal contributes 40,036 MW of the total generated capacity followed by hydro generation with 3,573 MW [7].

Type	Capacity (MW)
Coal	40,036
Gas turbine	3,449
Hydro	3,573
Wind	2,096
Nuclear	1,860
Solar PV	1,479
Solar CSP	400
Landfill gas	7.5
Imported Hydro	1,500
Total	52,811

Table 1.1: Generated capacity in South Africa [7]

There is huge potential for wind power penetration into this generation mix. However, the intermittent nature of wind presents several operational and control challenges that need to be addressed, in order to achieve greater wind power penetration into SA's regulated electrical environment. One of the major control challenges with complex interconnected power systems incorporating unpredictable renewable energy sources, is load frequency control (LFC) and tie-line power stability. Most of the research into LFC and tie-line power stability is limited to deregulated electrical environments with identical generating systems in each area and control strategies based on classical control theory. Hence, there is need for further investigations.

1.3 Problem Statement

For wind power penetration to be financially feasible in SA, it must be integrated into the existing transmission and distribution infrastructure. Currently, SA's electricity generation is dominated by coal and the penetration of wind power into

the national grid remains comparatively low. The literature indicates that tie-line power instability, resulting from inadequate LFC of interconnected power systems is one of the main obstacles to greater wind power penetration.

When incorporating wind generation into existing power plants, LFC is one of the most critical control issues relating to power system stability and operation [12]. With the increase in size and complexity of modern power systems and the integration of renewable energy systems, inadequate LFC will deteriorate the frequency of the system. The system oscillations could spread into a wide area resulting in tie-line instability and system failure. The proposed solutions for LFC incorporating wind generation have not been practically implemented due to system operational constraints associated with existing power plants having thermal or hydro generation [13]. The effectiveness of control strategies, based on classical control theory, is limited in design and control efforts and thus does not satisfy the requirements of interconnected power systems incorporating renewable energy such as wind power.

1.4 Aims and Objectives

1.4.1 Aims of this Research

- To analyse the effectiveness of, the active power support from doubly fed induction generator (DFIG) based wind turbines and Flexible Alternating Current Transmission System (FACTS) devices, when employed in an optimal control strategy for LFC, in a two-area interconnected hydro-thermal power system. The FACTS devices incorporated in this research are thyristor controlled phase shifters (TCPS) and super conducting magnetic energy storage (SMES) units.
- To analyse the effectiveness of an optimal controller, employing a model predictive control (MPC) strategy for LFC, compared to a conventional integral controller, in a two-area interconnected power system with thermal generations in both areas. Both controllers are supplemented with the active

power support from DFIG based wind turbines in each area, a TCPS and a SMES unit.

1.4.2 Objectives for the Optimal Control Strategy

- To design an optimal controller for LFC, based on error minimization through full state vector feedback, for a two-area interconnected power system consisting of hydro generation in area one and thermal generation in area two.
- Develop the transfer functions for, the interconnected power system, the DFIG based wind turbines, a TCPS in series with the tie-line and a SMES unit installed in area two of the system.
- Conduct mathematical modelling of the optimal controller and derive the system vectors for the three models under investigation.
- Simulate the power system's dynamic responses to load fluctuations, for load frequency stability and tie-line power stability, with and without the active power support from DFIG based wind turbines and the FACT devices. All the simulations in this research are produced in MATLAB/SIMULINK 2019.
- Evaluate the performance of the LFC strategy by interpreting the performance index values, the eigenvalues, the closed loop feedback gains and the response times of the controller for state parameter variations.

1.4.3 Objectives for the MPC Strategy

- To design and compare a MPC strategy with a conventional integral controller, for LFC in a two-area interconnected power system, consisting of thermal generations in each area, supported by DFIG based wind turbines, a TCPS connected in series with the tie-line and a SMES installed in area two.
- Develop the transfer function model of the system under investigation.
- Simulate the power system's dynamic responses, to sudden load fluctuations, system parameter variations and generation rate constraints, to investigate the frequency and tie-line power stability of the power system.

- Evaluate the performance of the MPC compared to the conventional integral controller, by analysing the graphically results obtained from the simulations.

1.5 Research Outputs

Published Journal Paper

D Chetty, G Sharma and I Davidson, “Active Power Regulation of the Power System considering DFIG based Wind Power in coordination with TCPS-SMES”, International Energy Journal, vol. 19, pp. 189–198, 2019.

Journal Paper Under Review

D. Chetty, G. Sharma, and I.E. Davidson, “Application of Optimal Control for Wind Integrated Power System with TCPS-SMES,” Internal Journal of Engineering Research in Africa.

1.6 Dissertation Structure

- **Chapter one** provided the context and motivation for the research. It focused on the generation capacity in South Africa, future generation plans and South Africa’s commitment to renewable energy. It also provided the aims and objectives of the research with regards to the LFC strategies being investigated in this research.

- **Chapter two** provides the literature reviewed in this research with respect to renewable energy penetration, hydropower, wind energy, DFIG based wind turbines, FACT devices with emphasis on TCPS and SMES units and classical LFC theory.

- **Chapter three** provides a review of optimal control strategies in LFC. It presents the design, modeling, simulation and analysis of an optimal controller, for a two-area interconnected hydro-thermal power system with and

without, utilising the active power support from DFIG based wind turbines, a TCPS and a SMES unit. The chapter concludes with a discussion of the results, obtained from the simulations.

- **Chapter four** provides a review of MPC strategies in LFC. It presents the design, simulation, analysis and comparison of the MPC to an integral controller, for a two-area interconnected thermal power system utilising the active power support from DFIG based wind turbines, TCPS - SMES units. The chapter concludes with a discussion of the results, obtained from the simulations.

- **Chapter five** is the concluding chapter which provides a summary of the research and recommendations for possible future research.

CHAPTER TWO: LITERATURE VIEW

2.1 Renewable Energy Penetration

There are three categories that energy sources are generally divided into: renewable, nuclear and fossil fuels [14]. Fossil fuels are the most widely used energy resources, however, there is a global shift away from fossil fuels due to the negative impact it has on the environment and global warming. Nuclear resources are surrounded by negative perceptions and controversy which hinders it's viability [15]. Geopolitical factors, decommissioning of nuclear facilities, radioactive waste material and reactor safety are some of the major concerns regarding nuclear power generation. There were 9,6 GW of nuclear development plans in the IRP 2010 [2]. However, in 2018 the SA government abandoned these plans and stated that it would focus on renewable energy resources instead and there will be no new nuclear capacity developed by 2030 [16]. This has opened the door for the rapidly growing renewable energy sector in South Africa.

In 1998 renewable energy only contributed 2 % to the total global energy capacity, while in 2017 this figure rose to approximately 24 % [17]. Though still comparatively low, the renewable energy sector is continuously growing. In [17], renewable energy technologies are categorised as mainstream technologies and emerging technologies. The mainstream technologies are established technologies with rapidly growing penetration levels. These include geothermal energy, biomass, solar energy, wind energy and hydropower. Hydropower and wind energy generation, which are the two renewable generation sources incorporated in this research, are briefly discussed below.

2.2 Hydropower Generation

Of the total installed generation capacity in South Africa, 3573 MW is generated from hydropower [7]. 90 % of the feasible large scale hydro potential has already been developed [18]; however there is significant potential for new small to

medium scale hydropower development under the REIPPPP. The advantages of these small to medium scale schemes are that, they can also be used for supplementary water projects and they can be combined into hybrid power systems, incorporating other renewable sources such as wind generation. It is for this reason, that a hydro generation supported by wind integration is considered for one of the investigations in this research. Also, significant opportunities exist for South Africa to import more hydropower from its neighboring countries. There is significant hydropower potential in the Zambezi River and the Congo River (Inga Falls). If these potentials are realised it could be integrated with wind power generation and South Africa can move a step away from its dependence of coal.

2.3 Wind Power Generation

The wind energy industry is experiencing rapid expansion due to the increase in size and quantity of wind generation systems installed globally [19]. Wind energy conversion system (WECS) could either be grid connected, contributing to the total power supplied by the distribution system, or they could be stand-alone systems. Due to the growing penetration of grid connected WECS, it is necessary to investigate their performance in interconnected power systems, especially in regulated environments. A WECS basically consists of a transformer, power electronic convertor, generator, gearbox and a turbine. Wind energy is captured by the turbine blades, converted into mechanical power and transferred via the gearbox to a three phase generator, where it is converted to electrical power. The maximum power obtained from the wind is presented in [20]:

The energy flow rate is:

$$P = \frac{dE}{dt} = \frac{1}{2} v^2 \frac{dm}{dt} \quad 2.1$$

Mass flow rate is given by:

$$\frac{dm}{dt} = \rho A \frac{dx}{dt} \quad 2.2$$

Where:

p is air density (kg m^{-3});

A is blade sweep area (m^2);

$\frac{dx}{dt} = v$ = wind speed (m/s)

Therefore:

$$\frac{dm}{dt} = \rho A v \qquad 2.3$$

From equation (2.1) wind power can defined as:

$$P = \frac{1}{2}\rho A v^3 \qquad 2.4$$

Taking Betz Limit into consideration that the maximum efficiency of a wind turbine cannot exceed 59 %; power coefficient is C_{Pmax} = 0.59

Hence:

$$P = \frac{1}{2}\rho A v^3 \; x \; 0.59 \qquad 2.5$$

The integration of a WECS in an interconnected power system with an alternate generating source is illustrated in figure (2.1).

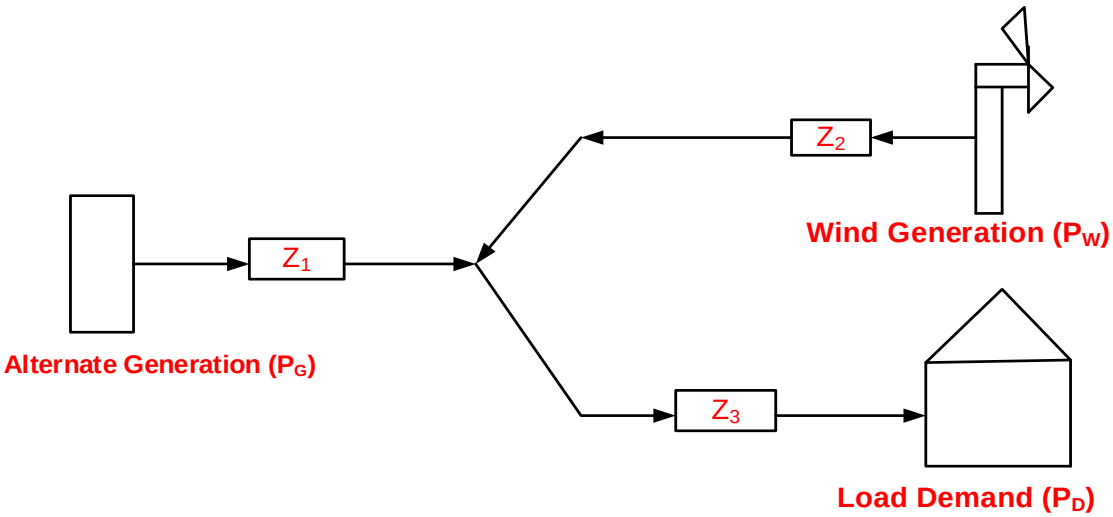

Figure 2.1: Illustrative power system

There will always be balance in the power system, as:

$$P_G = P_D + P_L - P_W \qquad 2.6$$

Where P_L is the power losses in impedances Z_1 - Z_3;

From equation (2.6), it is noted that power cannot be stored in a power system. Therefore, a change in load demand or wind generation must be simultaneously compensated by other sources within the interconnected power system. Wind generation depends considerably on the type of wind turbine that is used. Wind turbines are categorised as follows in [21]:

- **Fixed-Speed Wind Turbine (FSWT)**: the turbine speed is constant and independent of the wind speed. The gearbox ratio, generator design and grid frequency regulates the turbine speed. It is connected directly to the grid coupled with an induction generator. The reactive power is controlled by soft starters and capacitor banks. The capacitor banks provide static compensation only and therefore, cannot actively participate in reactive power control. Although reliable and simple, the power quality and system stability is poor because the variations in wind speed, is transferred to the grid through the constantly changing mechanical torque [21].
- **Variable-Speed Wind Turbine (VSWT)**: operates in a relatively wide speed range allowing for the generator torque to be maintained constant. A synchronous generator or an induction generator may be used with a VSWT. The generator can operate below or above synchronous speeds because the fluctuating wind speeds are transferred to the rotor of the generator. It is connected to the grid via power electronic converters which constantly adjust the generator speed, thereby regulating the generator frequency and grid voltage [22]. It can actively participate in the reactive power control resulting in better power quality and greater system stability. But it is complex in design and expensive, compared to FSWT and the additional power convertors that are required results in increased system losses [23].

In a WECS, the wind energy is converted to mechanical power by the wind turbines, which is then converted to electrical power using three phase generators. The different generators that may be used are briefly reviewed in sections (2.4 – 2.6).

2.4 Synchronous Generators

In a synchronous generator a rotating magnetic field is created by applying DC current to the rotor windings. The rotating field induces a three phase voltage in the stator windings which is transferred to the grid. Synchronous generators have a low rotational synchronous speed, therefore they are commonly used for VSWT applications [24]. Pitch control is not required, resulting in lower cost and less stress on the turbine and generator. Their operating speed must be above synchronous speed to run in generating mode. Direct drive of the turbine and generator can be achieved by eliminating the gearbox. This is achieved by using synchronous generators with a salient-pole rotor consisting of multiple poles. Multipole synchronous generators can supply voltage at grid frequency. A reactive magnetizing current is not required in synchronous generators. The excitation voltage for the rotor winding is supplied by an external DC source or an AC/DC convertor. A permanent magnet synchronous generator (PMSG) or a wound-rotor synchronous generator (WRSG) may be used.

In a PMSG, the rotor is a permanent magnet pole system and the stator is usually wound. Energy dissipation is not required for the excitation [24]. Full power conversion using power convertors regulate the generator frequency and voltage to match that of the grid [25]. The PMSG is associated with huge power losses due to the power convertors. In a WRSG, the rotor is excited by DC current from the slip rings and brushes while the stator is directly connected to the grid. The direct current creates an excitation field in the rotor windings which rotates at synchronous speed. The number of poles and the rotating field frequency determines the synchronous speed [26]. The large number of poles required, to maintain desired frequency levels, makes the WRSG physical big and therefore expensive. Synchronous generators are generally used in conventional power plants coupled with steam or hydro turbines. This system model is illustrated in figure (2.2).

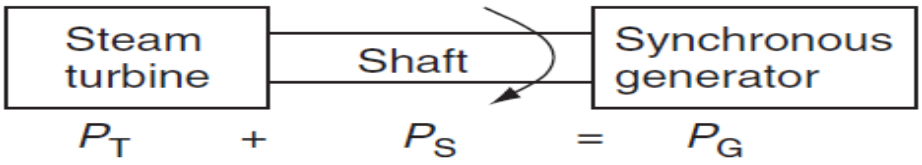

Figure 2.2: Power in a conventional power plant

The rotor of the generator is driven by the rotating turbine. The power supplied by the turbine is P_T and the combined power delivered from, the stored kinetic energy of the rotating turbine, shaft and rotor is P_S. Under normal operating conditions P_S is zero. P_G is the power supplied to the grid. Power generation will increase when the load demand increases. The initial increase in power is produced from the stored kinetic energy, P_S. This results in a decrease in the speed of the turbine–shaft–generator. The decrease in rotor speed results in a decrease in the grid frequency. Therefore, a sudden load increase causes the grid frequency to decrease.

Synchronous generators are ideal for wind power systems because total power control can be achieved. The diagram of a WECS using a multipole synchronous generator is shown in figure (2.3).

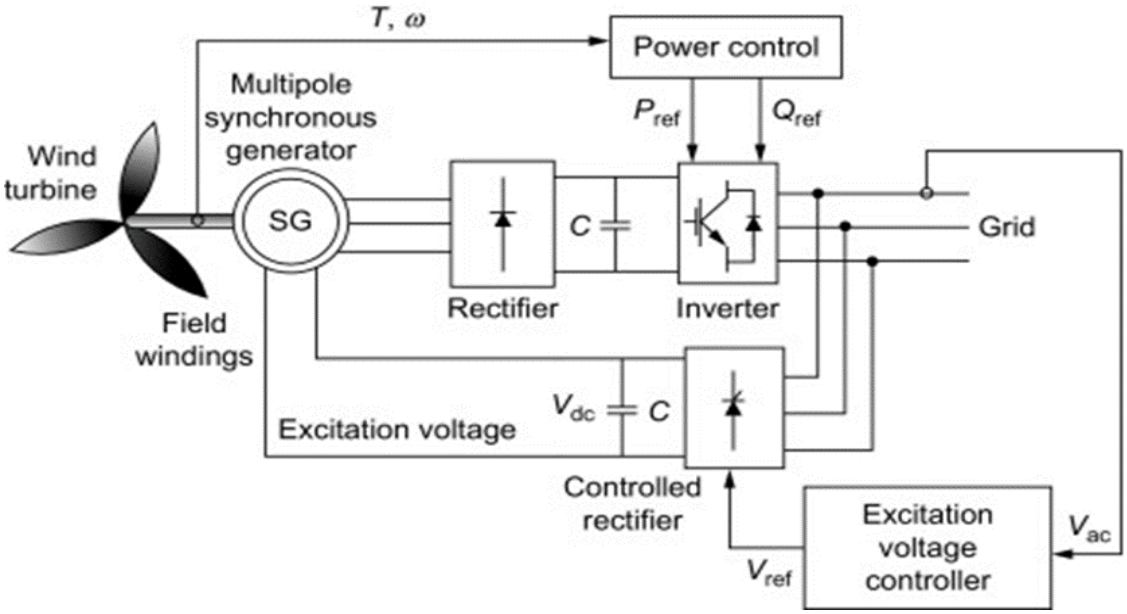

Figure 2.3: WECS using a multipole synchronous generator [24].

Power is supplied to the grid via power electronic convertors, but the additional power losses associated with these power convertors, the mechanical complexity, the physical size and the cost implications make it less desirable in WECS compared to induction generators [27].

2.5 Induction Generators

Induction generators are the most extensively used generators in the wind energy industry because of its high energy capture with comparatively simple controls. The advantages of the induction generators compared to synchronous generators are summarized in [28]:

- a reduced power to weight ratio;
- high life span, (above fifty years);
- low maintenance;
- mechanically simple and
- comparatively cheaper.

The rotor is mechanically rotated above synchronous speeds to produce power. Instead of using a permanent magnet system, the excitation is created by an external source using the reactive power [29]. The reactive power is supplied by the grid for the generator's magnetisation. Induction generators are either wound-rotor (WRIG) or squirrel-caged (SCIG).

The SCIG is coupled to the turbine via a gearbox and the stator is directly connected to the grid via a transformer. The rotor speed is directly proportional to the grid frequency. SCIG are coupled with FSWT resulting in wind speed variations being transferred to the grid due to the changing torque. Power system instability is likely to occur at high wind speeds due to the excessive active power generated resulting in abnormally high reactive power absorption from the grid. The full load power factor is very low because of the reactive magnetising current required by the stator during start up. To reduce the reactive power absorbed

from the grid, capacitor banks are generally used to supply the reactive power that is required [30]. Figure (2.4) shows the basic configuration of a SCIG connected to the grid.

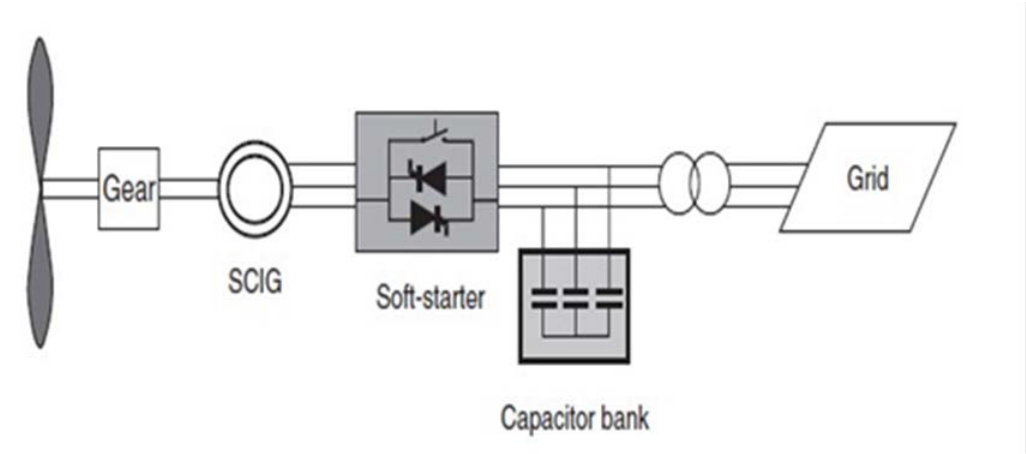

Figure 2.4: Grid connect SCIG [21]

The WRIG differs from the SCIG in that the stator and rotor can be independently excited. It is generally coupled with VSWT. The WRIG can either be an OptiSlip induction generator (OSID) or a doubly fed induction generator (DFIG) [26]. The OSID, also known as a variable resistance induction generator is shown in figure (2.5).

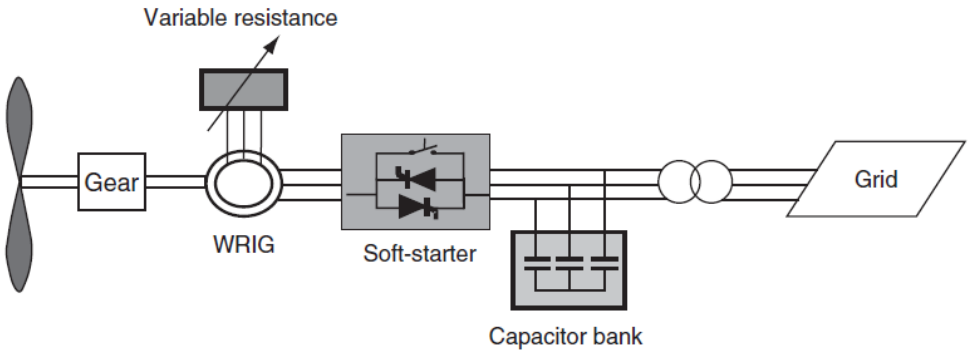

Figure 2.5: Variable resistance induction generator [21]

It has a variable resistor combined to the rotor circuit. The rotor resistance is varied to adjust the slip and the stator is connected directly to the grid. Compared to the SCIG, the OSID is simple in design and mechanical construction, with limited power variations. However, the OSID has a few disadvantages; the

reactive power control is ineffectual; the speed range is proportional to and limited by the variable resistor and the variable resistor contributes to considerable power losses. It is for these reasons that the DFIG has gained prominence in the wind industry. A detailed review of the DFIG is presented in the next section and its mathematical modelling and transfer function is presented in chapter three.

2.6 Doubly Fed Induction Generators

In a DFIG, the stator and rotor are connected to the grid independently. The rotor is connected to the grid through power electronic convertors and the stator is directly connected to the grid, as shown in figure (2.6).

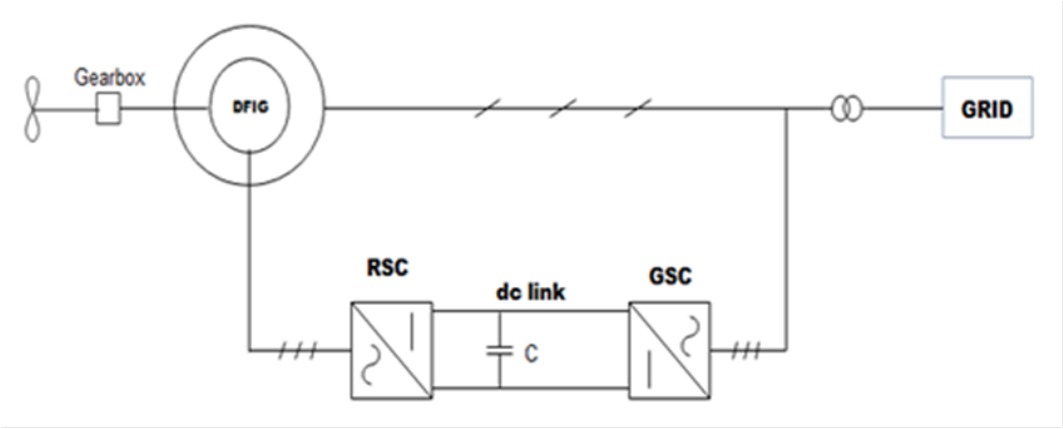

Figure 2.6: Grid connected DFIG [31]

Wind energy is captured by the blades of the wind turbine which is transferred to the DFIG through a gearbox. The DFIG transfers electrical power to the grid through the stator windings, and back-to-back converters from the rotor windings. The power delivered by the rotor and stator can be calculated as follows:

$$P_R = sP_S \qquad 2.7$$

Where

P_R is the rotor power

P_S is the stator power

s is the slip

Therefore the mechanical power supplied to the generator can be expressed as:

$$P_m = (1 + s)\, x\, P_S \quad 2.8$$

The grid supplies the stator voltage and the convertor supplies the rotor voltage. The converter supplies the rotor with current of variable frequency to compensate for the difference between the turbine frequency and the grid frequency. The DFIG operates at two discrete frequencies; rotor side frequency and stator-grid frequency. The rotor frequency is proportional to the difference between the rotor speed and stator frequency. The active power is distributed between the rotor and stator at the approximate ratio of the slip frequency. The rotor side frequency is continuously adjusted to compensate for the variable turbine speed which may cause variations between the turbine frequency and the grid frequency. The convertor on the rotor side (RSC) regulates the active and reactive power flow while the convertor on the grid side (GSC) ensures that the RSC operates and unity power factor by maintaining a constant DC link voltage. The DFIG is able to maintain optimal operation at varying speeds, (super-synchronous and sub-synchronous speeds) to supply power to the grid. This is a major advantage of the DFIG that the sudden changes in wind speed do not affect its performance. At super-synchronous speeds, power is supplied to the grid from the rotor via the convertors. At sub-synchronous speeds power is supplied to the rotor from the grid. While the rotor is operating at varying frequencies, the stator continues to supply power to the grid at the grid frequency.

At high wind speeds, the RSC employs a maximum power tracking (MPPT) algorithm to control the turbine speed within desired limits while still generating maximum power [32]. By controlling the operating point of the turbine, the power generated during high wind speeds is reduced, therefore the mechanical stresses on the turbines are significantly lower. In [32-33], various methods for MPPT are discussed. The reactive power flow between the grid and the generator is controlled through the convertor. At low wind speeds when there is low reactive power compensation, the RSC controls the reactive power to maintain the voltage across the stator [34]. The RSC injects current into the rotor to control the rotor speed. This ensures that the stator voltage and frequency is stable and optimal power generation is maintained. The reactive power is transferred to the stator

via the GSC, while the rotor excitation current is independently controlled by regulating the active and reactive power.

A significant benefit of the DFIG is highlighted in [34]; the RSC deals with approximately 25 % of the rated power which reduces losses, resulting in reduced cost compared to wind turbines that employ full-power convertors. An investigation between DFIG based wind turbines and wind turbines that employ full-power convertors is conducted in [35]. The investigation demonstrated that the power produced by the turbines, that employ full-power convertors is significantly lower, compared to the power produced by the DFIG based wind turbines. The bi-directional power flow between the grid and the rotor is controlled in direction and magnitude to ensure that the generated power is at a constant voltage and frequency, thereby maintaining system stability. A stability analysis of a wind farm is conducted in [36], where the conventional synchronous generators are replaced with DFIG. The model analysis showed that the DFIG-based wind farm delivers better frequency responses when it replaced the conventional synchronous generators.

In a system that employs DFIG based wind turbines, the inertia of the turbine (mechanical system) is decoupled from the generator (electrical system). Therefore, the kinetic energy of the turbine cannot actively support the generator in response to frequency variations, resulting in poor system frequency control. To compensate for frequency variations, due to changing wind speeds or changing load demands, power electronic controllers are used which interface between the wind energy system and the grid. The following frequency control methods, in power systems using VSWT, are discussed in [37]:

- inertial control
- pitch control or speed control (power reserve control)
- communication method control

This research demonstrated that system frequency can be stabilised if wind turbines actively engage in system inertia requirements. In [38], an additional

control loop is employed to the DFIG controller, with a supplementary power reference point based on the rate of change of the network frequency and the network inertia. The system frequency is constantly monitored and the primary frequency (rotor side) is supported by the DFIG based wind turbines, releasing additional kinetic energy into the system which maintains overall system stability. A frequency control support function is employed in [39], for a two area interconnected power system. The controller provides proportional response to any variations in the system frequency, by using the kinetic energy of the DFIG based wind turbines. This investigation demonstrated that by installing DFIG based wind turbines in each area, system stability is significantly improved.

The participation of DFIG based wind turbines in frequency control by means of the system's inertial response and the governor settings are investigated in [40]. In the case study conventional synchronous generators are replaced with DFIG. The study demonstrated the effective support of DFIG in maintaining desired system frequencies. In [41], the active support of DFIG base wind turbines, employing a modified inertial controller with fast control reactions for frequency variations, due to sudden load changes, is demonstrated with positive results. A de load optimum power extraction curve is used in [42], to control the active power supplied by the DFIG based wind turbines during frequency fluctuations. Using pitch control and static convertors to adjust the rotor speed, this research demonstrated that the active power can be adjusted in accordance with a de loaded optimum power extraction curve. According to this research, the disadvantage of using the de loaded optimum curve method is that maximum power cannot be generated by the DFIG. Two vital concepts for employing VSWT in WECS are presented in [43]:

- Using a DFIG with back-to-back voltage source convertors to feed the rotor windings.
- Using a directly driven synchronous generator which is connected to the grid via a voltage source converter and a diode rectifier.

DFIG based wind turbines has the advantage of being able to actively participate

in system frequency variations which results in improved system stability, during changing wind speeds and changing load demands. It provides significantly better responses to frequency variations at much lower costs. There is vast literature available on the active power support of DFIG based wind turbines in response to frequency variations. However, research on the support of FACTS devices, in conjunction with DFIG based wind turbines, for LFC and power system stability in interconnected hybrid systems, is limited in scope. There is a need to investigate the merits of combining FACTS devices in conjunction with DFIG based wind turbines in an optimal control strategy for LFC and tie-line power stability. A review of the FACTS devices relevant to this research is presented in section (2.7).

2.7 FACTS Devices

Power system stability, improved reliability and low costs are major concerns regarding transmission and distribution of interconnected hybrid power systems. Transmission and distribution stability is drastically reduced if any transmission parameters such voltage and frequency, deviates from their nominal operating values. In an interconnected power system, system instability in one control area may spread into the transmission and distribution system affecting other areas or the entire network. During fluctuating operating conditions in any area, interconnected power systems must be able to maintain steady-state operating conditions in all areas. To improve transmission reliability, FACTS devices were developed to maintain system parameters at optimal operating values. FACTS devices are power electronic devices that are used to enhance power transmission capabilities of electrical power systems, thereby eliminating the need to add new transmission lines to the network [44]. FACTS technology assists in maximizing the use of existing transmission systems by increasing the performance of power systems [45]. Therefore when new power plants are built they can be integrated into the existing electrical infrastructure, thereby reducing costs and negative effects on the environmental. FACTS devices deliver rapid responses to system variations to maintain desired voltage and frequency parameters thereby preserving power system stability [46].

The positive impact of FACTS devices used in power system stability, incorporating renewable energy generations is highlighted in [47]; they provide rapid compensation for, voltage, frequency and active and reactive power variations to improve transient system stability. Induction generators absorb reactive power, traditionally, reactive power compensation is supplied by Load Tap Changes (LTC) and capacitor banks. In [48], FACTS devices are presented as an alternate strategy in moderating poor power flow and excessive reactive power absorption. Emphasis is placed on the positioning of FACTS devices in [49], to reduce system power losses and improve power system stability. FACTS devices are be classified as follows in [49]:

- **Shunt-connected controllers**: these controllers regulate the current in a power system. The controllers are able to inject current into the tie-line or absorb current from the grid. They may be used to provide capacitive compensation or inductive compensation. A shunt capacitor is used for power factor correction by absorbing current leading the grid voltage. Shunt inductors are connected across transmission lines to increase the power transfer capabilities.
- **Series-connected controllers**: these are connected in series with tie-lines to control the voltage, thereby regulating the power flow. The impedance of the line could be increased to decrease the active power transmitted, or decreased to increase the active power that is transmitted. This also results in a corresponding change of the reactive power.
- **Combined series-shunt controllers**: these controllers are a combination of series controllers and shunt controllers. The series controllers supply voltage to the transmission line and the shunt controller injects current into the line.
- **Combined series-series controllers**: these are a combination of various series controllers that are positioned and employed in a strategic manner to provide active power regulation and reactive power compensation.

Due to the robustness of FACTS devices, the research in [49] provided a generic algorithm to determine the optimal positioning of the various FACTS

configurations. The investigation also highlighted that there is insufficient research into wind energy optimization methods, to achieve greater wind energy penetration levels. The application of FACTS devices such as the redox flow battery (RBF), the battery energy storage system (BESS), superconducting magnetic energy storage (SMES) units, static synchronous series compensator (SSSC) and thyristor control phase shifter (TCPS), are available in the literature [50-52, 56-58, 61-63].

Energy storage devices, combined with power electronics controllers, are employed in interconnect power systems to improve power system stability. These devices improve the performance of LFC resulting in enhanced system stability. Energy storage devices for LFC require further investigations because they have not been adequately investigated. The RBF is a fast acting energy storage device, in conjunction with the kinetic energy of generator rotors, a RBF can also provide stored energy during sudden load demand fluctuations. The RBF releases stored energy, through an inverter-rectifier conversion system, which minimizes electromechanical oscillations in the power system. The positive effects of the RBF in LFC are demonstrated in [50]. However, this investigation revealed that the RBF only has a positive stabilising effect in the control area in which it is positioned and installing a RBF in each area of an interconnected power system is not financially feasible. The BESS is another energy storage device that could also be employed in power systems to reduce electromechanical oscillations. Apart from the kinetic energy of the rotor, a BESS can provide additional energy during low power flow. In [51-52], the impact of the BESS for LFC are investigated. The investigations demonstrated the positive impact of the BESS, in responding to sudden fluctuations in load demand in a network, by reducing the frequency and tie-line power variations. However, the maintenance requirements, low discharge rates and increased response times for power flow reversal are major disadvantages of the RBF and the BESS. These disadvantages drove the development of the SMES units as an effective FACTS device, for frequency control and tie-line power stability in interconnected power systems.

SMES units are desirable for LFC because of its rapid response times and its ability to simultaneously control active and reactive powers. The author in [53] reports that large-scale SMES research, is currently being funded by the US Department of Energy. In a SMES unit energy is stored in the magnetic field. The magnetic field is created in a superconducting coil by circulating DC current. By discharging the coil, energy is released back into the network. Inverter-rectify convertors are used to convert AC to DC when the coil is charging and DC to AC when power is fed back into the system. The superconducting coil charges and discharges almost instantaneously because there is no energy conversion, therefore, the SMES responds rapidly to system variations. The response times are only limited by the time taken for the DC power to be converted to AC [54]. SMES units are generally installed at power system outputs where they may be used to compensate for, peak load demands, limit voltage instability, and reduce frequency oscillations, thereby improving power quality and system stability [55].

In [56-58], S.C. Tripathy et al. investigates the performance of SMES units installed in interconnect power systems. In [56], it observed that when an adaptive SMES controller is employed, the system performance is unaffected to system parameter variations. The effect of SMES on LFC, considering system nonlinearities like governor dead-band and reheat constraints are investigated in [57]. The case model employed a small-capacity SMES unit. These investigations demonstrated that a small-capacity SMES is effective in LFC, which is significant because SMES units are very expensive but they could be easily resized thereby reducing costs. The performance of the system considering load fluctuations is evaluated in [58], using a sampled data mode in conjunction with a small capacity SMES unit. The simulated results demonstrated the effectiveness of SMES in response to frequency variations due to changes in load demand. LFC of a hydro-thermal interconnected power system with installed SMES units is investigated in [59], the investigation demonstrated that the dynamic performance of an interconnect power system is improved by SMES devices. However, this investigation also revealed that SMES units only have a positive impact in the

area in which the unit is installed and has negligible impact in other control areas. SMES units installed in both regions, of a two area interconnected power system, improve the system's dynamic performance when sudden load fluctuations occur in either area. However, SMES units are expensive and installing them in different areas of an interconnected system is not financially feasible, therefore, the need to investigate other FACTS devices that may be employed in conjunction with SMES units.

Due to the constant advancements in semi-conductor devices, power transmission technologies have developed rapidly in the last few decades. One application these technologies is high voltage direct current (HVDC) transmission lines. Several problems of interconnected power systems can be eliminated by using HVDC technology. However, HVDC technology is not considered in this research because most of the existing transmission lines in South Africa are AC and for renewable energy integration to be financially feasible it must be integrated into the existing electrical infrastructure.

A SSSC is a series connected voltage-sourced compensator that controls the active and the reactive power in transmission lines in order to improve power system stability. The output voltage and line current is controlled independently for the purpose of regulating the reactive voltage across the line, thereby controlling the active power that is being transmitted. When the voltage lags the line current, the compensator acts as a series capacitor and when the voltage leads the line current, the compensator acts as a series inductor [60]. In [61], SSSC for an interconnected power system consisting of thermal reheat turbines, is investigated. The investigation assumed large load fluctuations in area one resulting correspondingly large frequency variations. The investigation included governor dead band and GRC nonlinearities. This investigation demonstrated that SSSC is effective in maintaining tie-line power stability and desired system frequency, during sudden load changes.

The effectiveness of TCPS in power system oscillations is analysed in [62]. The research focused on how the TCPS operates, the robustness of a TCPS, and the optimal location for a TCPS in interconnected power systems. The analysis of this research concluded that, a TCPS provides extra stabilising support to system oscillations, that a TCPS could have different effects on different generators connected in the system, so they need to be designed in co-ordination with other controllers and a simple index model was proposed to determine the optimal positioning of TCPS in large interconnected power systems.

In [63-65], P. Bhatt et al investigates the combined effect of TCPS and SMES in different power system models. The effective response of a TCPS in conjunction with a SMES unit is demonstrated in [63]. In [64], the power system model is a multi-area interconnected power system with hydropower generation in each area. The investigation demonstrated that in hydropower generation systems, the frequency is very sensitive to sudden load variations because of the slow response times related to hydro turbines. However, by installing a TCPS in conjunction with SMES units in each area, the dynamic response of the system is significantly improved. The active performance of various system models using TCPS and SMES units is presented in [65] with positive results. It is observed from the literature survey that most of these investigations of TCPS and SMES units are limited to interconnected power systems having identical reheat or non-reheat turbines and little focus is given to interconnected power systems with different generating turbines that have vastly different characteristics, therefore, there is need for further research in this area.

The literature review informed the decision of employing a combination of TCPS and SMES units in the control strategies that are being investigated in this research. TCPS is just as effective as other series-connected controllers but they are comparatively cheaper. It controls the active power transfers between the tie-lines and other interconnected areas, thereby reducing frequency variations and maintaining power system stability in different control areas after sudden load disturbances. SMES units are the most effective storage devices currently

available. Although they are much more expensive than other storage devices, they are easily scale-able (resized) which would reduce costs and research is currently being conducted into the cooling of the superconducting coil which would also significantly reduce costs in the future [53]. The modelling and transfer function of a TCPS and a SMES unit is presented in chapter three. The successful implementations of FACTS devices, or a combination thereof, largely depend on the control strategies in which they are employed. The next section reviews the various LFC strategies.

2.8 Load Frequency Control Strategies

Interconnected power systems consist of multiple areas that are linked through tie-lines. The speed or torque of the generators in each area, need to be continuously adjusted to maintain desired system frequency. If sudden load fluctuations occur in one area resulting in frequency variations, the oscillations may spread into the tie-lines and other connected areas leading to power system instability. In large complex interconnected power systems LFC is a complex problem to solve, especially in interconnected systems that incorporate generations from unpredictable renewable energy sources.

LFC is one of the most essential control issues relating to power system operation and control [12]. There are numerous investigations into LFC strategies of interconnected power systems [66-74]. The first effort in the area of LFC for power systems was the use of a flywheel governor of a synchronous machine. The control effort was unsatisfactory and a secondary control was added to the governor. In [66], the control strategy is based on an integral cost minimisation of system state parameters which is defined mathematically. The control action is based on a state variable matric and the desired parameters are expressed mathematically in terms of cost minimisation. Mathematical algorithms, based on classical control theory, were developed in [67], but the control structures and system response models were unrealistically simple. Small signal analysis for LFC is employed in [68]. The control strategies employed in these investigations

that were discussed, constitutes the classical approach to LFC of power systems.

Power system frequency control, for a two area interconnected power system comprising of thermal turbines integrated with DFIG based wind turbines, is investigated in [74]. This research demonstrated that power system stability decreased under variable operating conditions and conventional controllers are inadequate in their design and control actions for large interconnected power systems. The performance of LFC designs based on classical or conventional control is restricted to systems having a single-input-single-output structure. However, a LFC design for interconnected power systems, is a design problem with multiple variables, therefore its effective study can be justified using modern control strategies.

The literature, [63-65, 75-77], proposes various optimal control strategies, for interconnected power systems. The results of these investigations revealed that optimal control techniques employing FACTS devices, or a combination thereof, drastically improves the system's dynamic responses and significantly limits system frequency variations within desired parameters, which leads to improved power system stability. However, most of the power system models used in these investigations employed identical hydro turbines or non-reheat, reheat thermal turbines in each region. Very little attention is placed on interconnected power systems with different generating turbines in each region that have vastly different operational characteristics. Hence, the need for additional investigations into interconnected power systems with different generation systems in each region. A further discussion into optimal control strategies together with the design, simulation and analysis of an optimal controller is presented in chapter three.

2.9 Conclusion

To conclude this literature review, the argument regarding dispersed electricity generation presented in [78], is evaluated. Experienced engineers, highly knowledgeable in complex power systems, are alarmed by the high penetration

levels of unpredictable energy sources such as wind energy, into existing distribution networks. But renewable energy enthusiasts, argue that renewable energy sources are a necessity in the combat against CO_2 emissions and the dominance of fossil fuels. The evidence of global warming due to CO_2 emissions from conventional power plants and the negative impact of fossil fuels on the environment is overwhelming. Also, the benefits of clean, sustainable renewable energy sources are beyond doubt, therefore the author of this thesis is in agreement with the later view. Hence, the relevance of this research in investigating optimal control strategies that may be practically implemented in interconnected power system incorporating wind generation.

CHAPTER THREE: OPTIMAL CONTROL STRATEGDY

3.1 Introduction

This chapter presents the design, simulation and analysis of an optimal LFC strategy, for frequency variations and tie-line power stability for a two area interconnected hydro-thermal power system. The control strategy is investigated with and without, the integration of wind power generations employing DFIG based wind turbines in each area, a TCPS and a SMES unit. The optimal control strategy is based on error minimization through full state vector feedback. This is achieved by developing a system state matrix combined with complete control feedback gains. The feedback gains are obtained through a control matrix and a disturbance matrix. An area control error (ACE) controller is installed in each area, which monitors state parameters through closed loop vector feedback and takes corrective action when the parameter values deviates from the reference values, in order to restore normal operating conditions of the system as quickly as possible. The effectiveness of the control action is analysed through the interpretation of the performance index (PI) values, eigenvalues, closed loop feedback gains and the results obtained from the simulations. The PI values indicate the error in the system, implying that there are system state parameter variations. The real and imaginary eigenvalues demonstrates the stability of the power system. The closed loop feedback gains of the controller demonstrate the effectiveness of the control action. The controller is simulated and the system dynamic responses are investigated for three power system models.

3.2 Review of Optimal Control Strategies

Various LFC strategies based on classical control theory, for power system stability of interconnected power systems, have been proposed. Controllers based on classical control theory are constrained to systems only having a single-input-single-output formulation [12]. In [67], control strategies based on conventional control theory are employed with unsatisfactory results. The conventional proportional integral (PI) controller is the most commonly used controller in interconnected power systems. It is comparatively cheap and

reliable; however, the PI controller produces fluctuating responses to system frequency variations [76]. Frequency stability is a control problem with multiple variables which can be solved using innovative control strategies such optimal control techniques. Controllers based on optimal control strategies yield significantly better performance results compared to that of conventional controllers.

The active support from DFIG, in coordination with TCPS and SMES for an interconnected power system is investigated in [63-65]. In [63], the optimal control strategy employed a particle swarm optimization (PSO) method, to achieve optimal integral control gains and parameter responses of the DFIG, TCPS and SMES. An improved version of the PSO is developed by the author in [64], called “craziness-based particle swarm optimization” (CRPSO). The performance of the CRSPO based optimal controller is compared to an optimal control strategy using a genetic algorithm in [65]. The investigation revealed that the CRSPO controller provided improved response times compared to the genetic algorithm controller.

In [68], the control strategy employed an Area Control Error (ACE) controller between the generation system and the grid. ACE is a linear combination of tie-line power and frequency variations in the power system. During load variations ACE regulates the corresponding tie-line power variations and frequency variations in order to restore normal system operating conditions as quickly as possible. An optimal controller for an interconnected system, based on full state feedback control is employed in [65] and the results demonstrated improved system stability for all the system models under investigation. A linear quadratic optimal controller (LQR) is investigated in [76]. This investigation employs an integral of a quadratic function of control inputs and system states, which is based on full state feedback control. In an LQR strategy the quadratic execution record is reduced to optimise the feedback gain matrix of the controller. An optimal strategy employing a sampled-data controller with a time-multiple performance index is evaluated in [65]. The author in [79], proposed an optimal control strategy based on output vector feedback. Practically, this control strategy is feasible

because it is relatively simple to obtain all system outputs. A control strategy employing DFIG and FACTS in [80], were designed by reducing the performance index matric of the system. The results demonstrated quicker transient responses to frequency variations. The effectiveness of the optimal control strategy depends on formulating an error value and finding the feedback gains corresponding to each state of the system which are easily attainable as outputs. The stability of the control action is evaluated through eigenvalue analysis in a closed-ring [79 and 80].

The active characteristics of wind generators are very diverse compared to ordinary generators. The inertial energy of the wind generator is inaccessible to support the system frequencies when load fluctuations occur. If the installed wind capacity is adequately accessible to supply acceptable inertial support, the unfavorable consequences of the load fluctuations can be minimised. The active support of the DFIG in frequency stability is analysed by frequency control feedback that reacts proportionally to frequency fluctuations and releases the kinetic energy stored in the blades of turbine accordingly for frequency stabilisation in the system. The “essence of emulation” inertial control (EIC) is developed in [74]. The EIC of a DFIG, employs a second control loop to adjust the control reference points as a function of, frequency change and the rate of frequency change. To produce maximum power, the controllers try to maintain optimal turbine speed. The system responses are further enhanced by employing FACTS devices.

In view of the literature reviewed in chapter two and the discussion above, this chapter subsequently presents the design of an optimal controller for load frequency control and tie-line power stability. The design is based on error minimisation through full state vector feedback and for interconnected power systems. The effectiveness of the designed control strategy is analysed with and without DFIG based wind turbines and TCPS-SMES, in restoring optimum system frequency, for sudden load fluctuations in an interconnected system. In section (3.3), the models used in this research are described.

3.3 Models under Study

Model 1 is a two area interconnected power system with hydro generation in area one and tandem compound non-reheat turbines in area two. The two areas are interconnected through an AC tie-line. An ACE controller is installed in each area between the generation system and the tie-lines. The data for the hydro plant and the thermal plant is given in Appendix A and Appendix C respectively. The transfer functions of, the controllers, the turbines, the governors and the generators in each area is presented in the model as shown in figure (3.1).

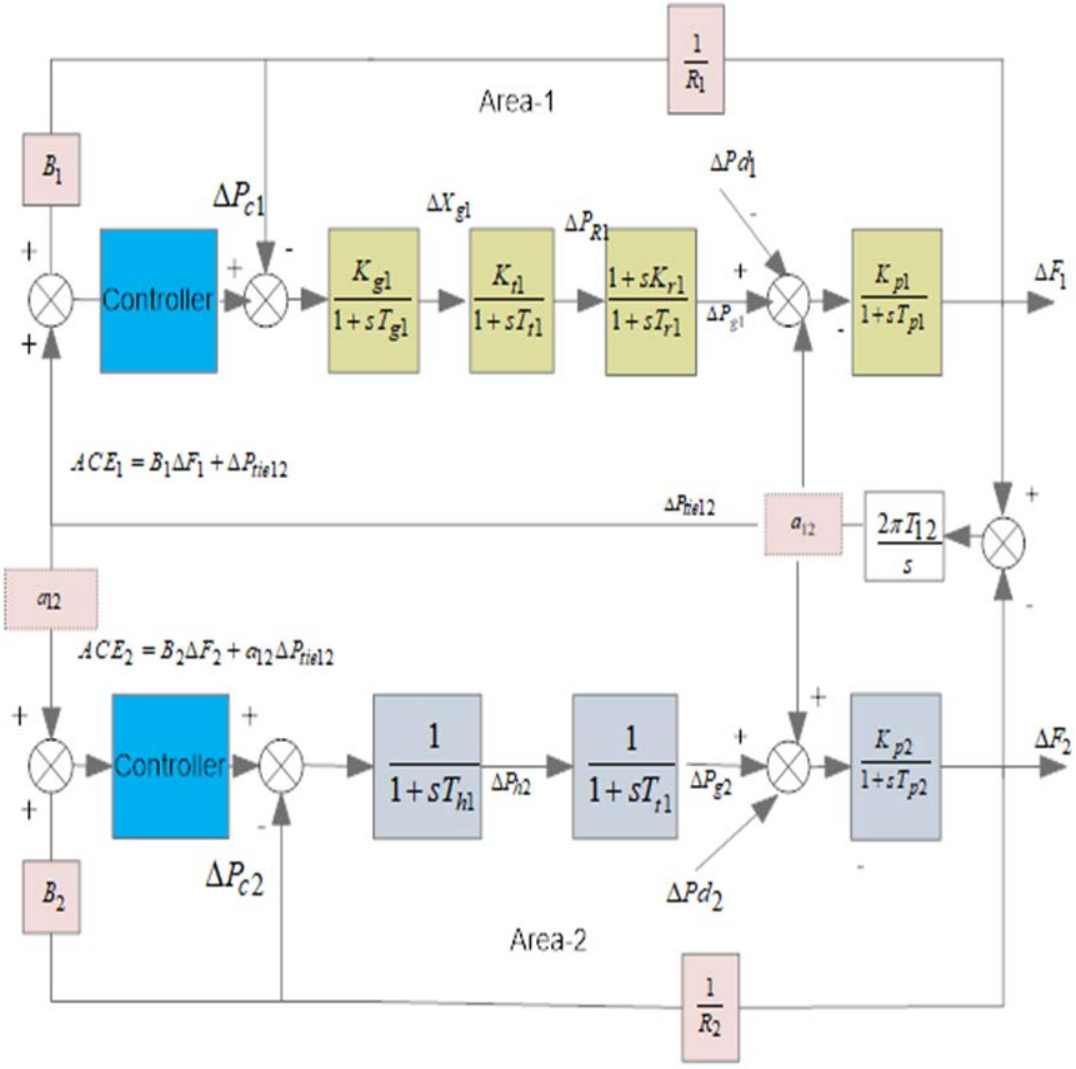

Figure 3.1: Two area interconnected system with hydro-thermal generation.

Model 2 is a replica of model one (hydro generation in area one and thermal generation in area two) but each area is now supported by wind generations employing DFIG based wind turbines. The data for the DFIG base wind turbines is given in Appendix B. The model in figure (3.1) is extended to include the transfer function model of the wind generation system incorporating DFIG based wind turbines in each area as shown in figure (3.2).

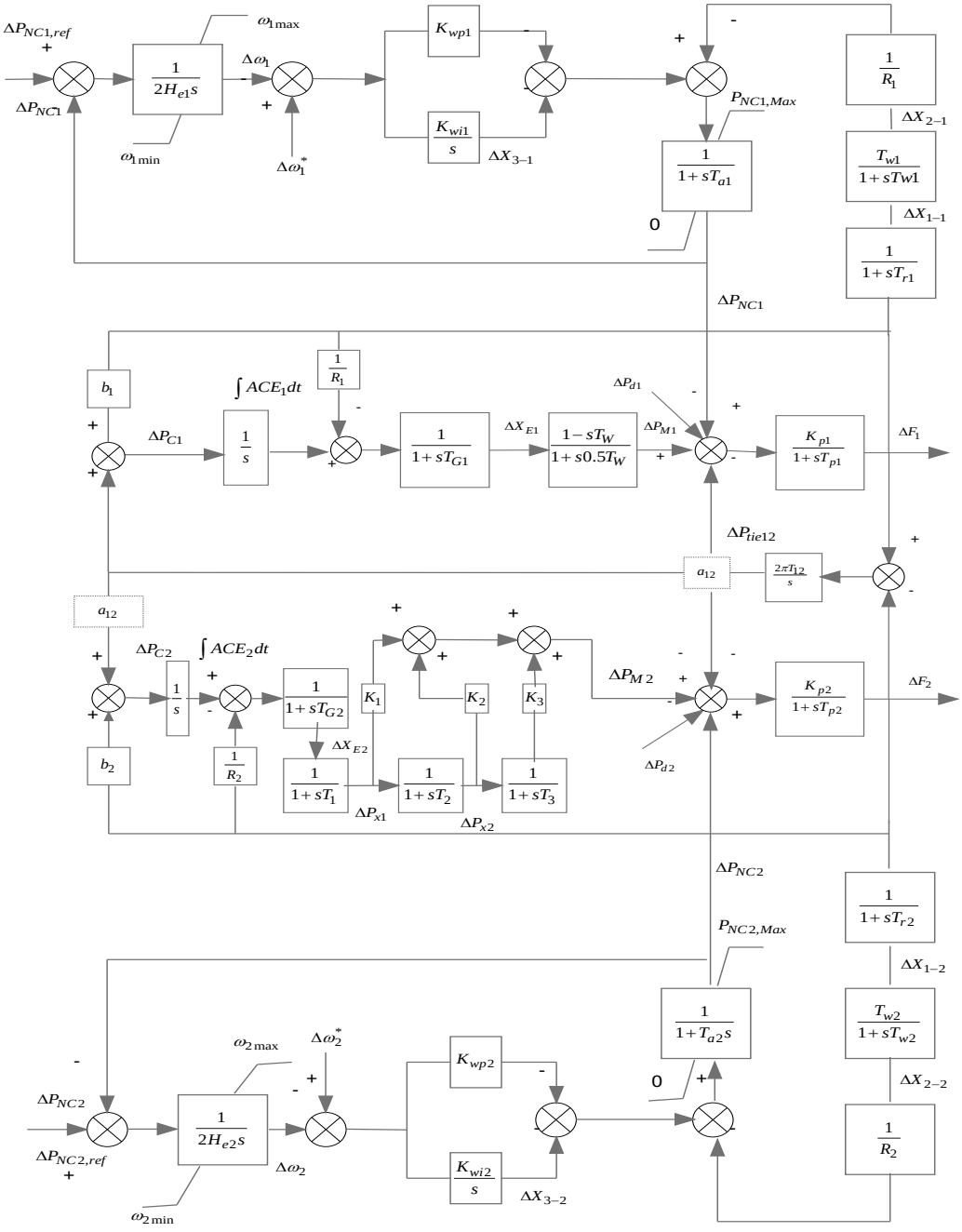

Figure 3.2: Two area hydro-thermal interconnected power system incorporating DFIG based wind turbines

Model 3 is a replica of model 2 (hydro in area one, thermal in area two supported by DFIG in each area) but the interconnected power system now employs a TCPS in series with the AC tie-line and a SMES unit located at the output terminal of area two of the system. The model shown in figure (3.2) is modified to include the transfer functions of the TCPS and a SMES unit as shown in figure (3.3).

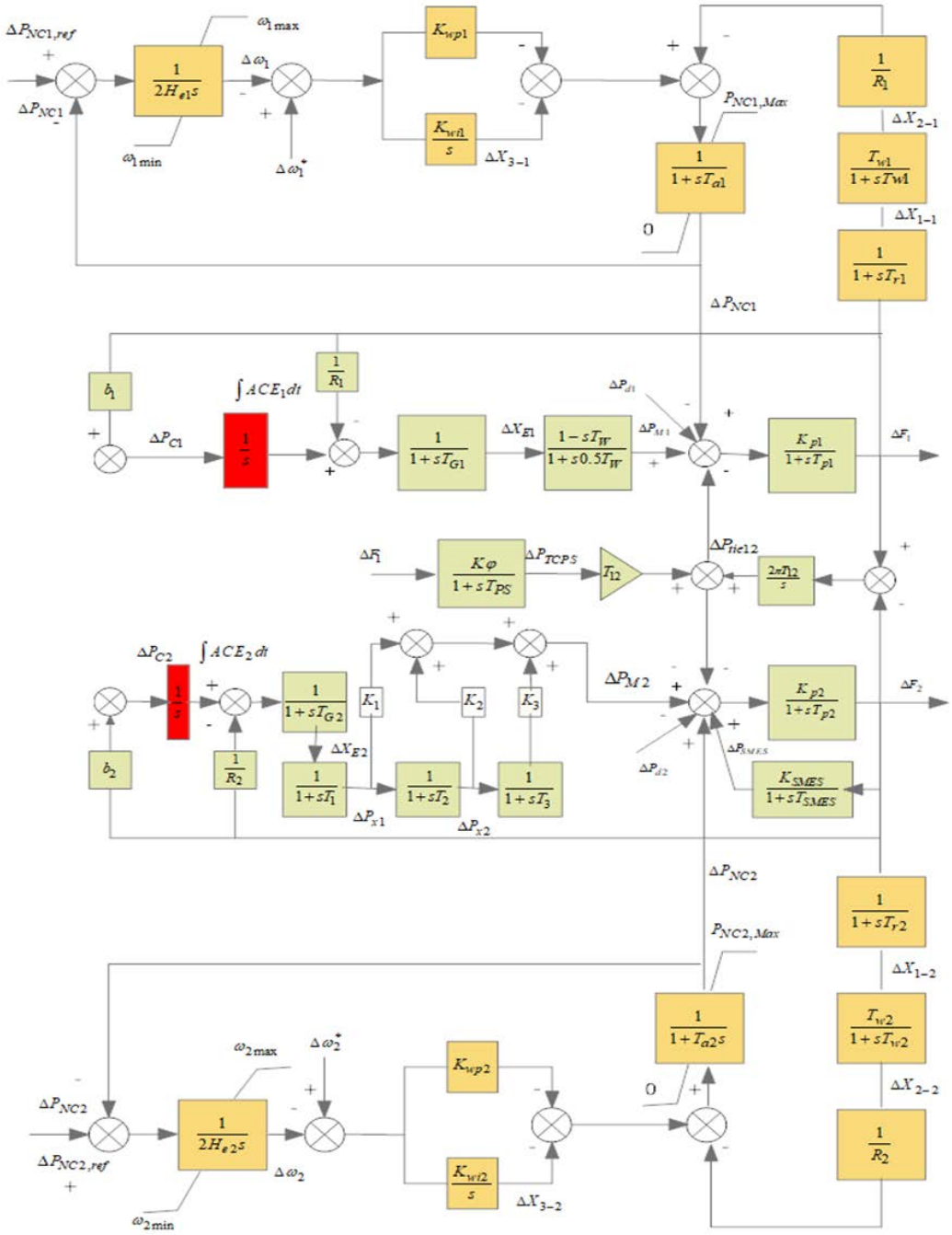

Figure 3.3: Two area hydro-thermal interconnected power system incorporating DFIG in conjunction with TCPS-SMES.

3.4 Modelling of a Wind Generation System incorporating DFIG

When wind generators are employed in frequency control, the wind turbines do not supply their accessible power directly into the system. Variable speed generators coupled to wind turbines, are used to extract the kinetic energy stored in the mechanical system. To achieve frequency control, DFIG based wind turbines can deliver power with variable mechanical speeds allowing for the kinetic energy to be extracted [42]. The transfer function for the model is shown in figure (3.4) and the system parameters are given in Appendix A.

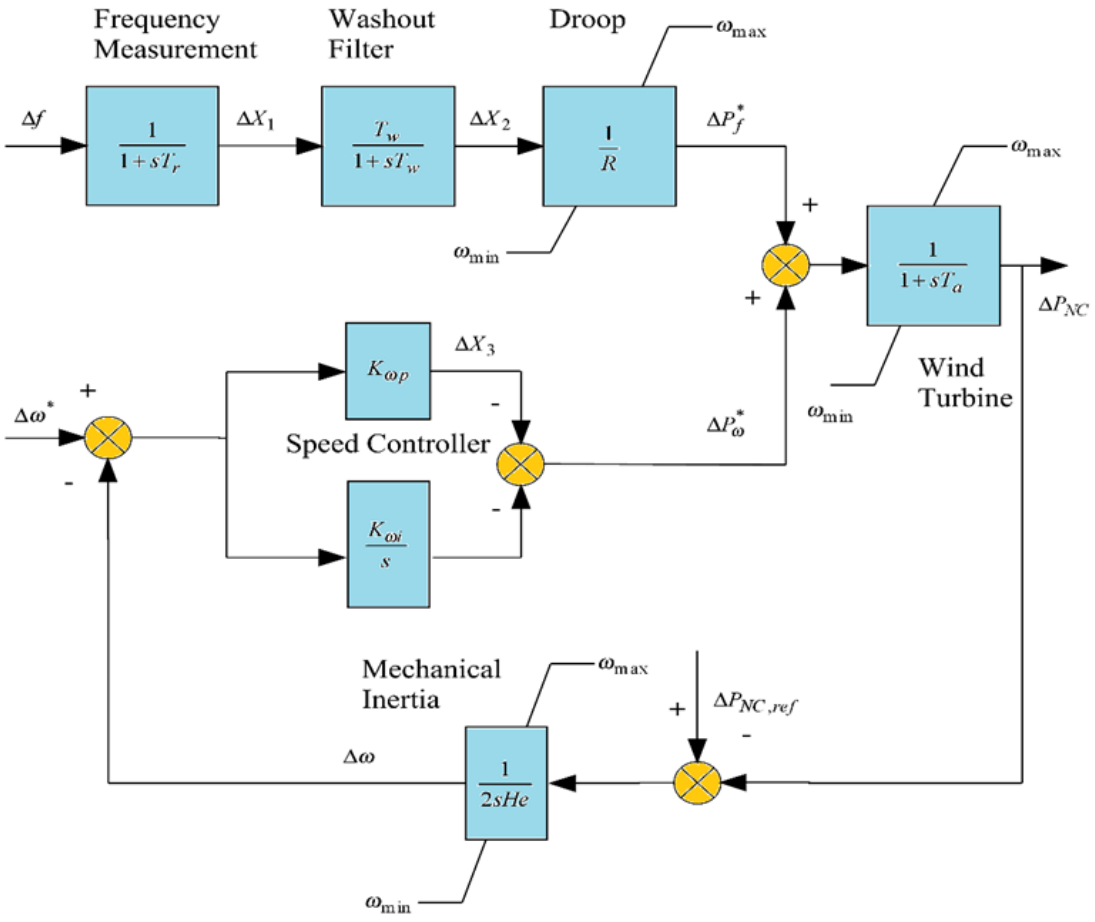

Figure 3.4: The transfer function of DFIG based wind turbine.

The development of the transfer function of a DFIG based wind turbine participating in frequency stability during load fluctuations is covered in [74]. The transfer function employs DFIG based wind turbines in each area for active power control. The model has the “essence of emulation” inertial control (EIC). For the EIC of a DFIG, a second control loop is utilized to adjust the control reference points as a function of, frequency change and rate of frequency change. To

produce maximum power, the controllers try to maintain optimal turbine speed. The controller provides a power reference point based on measured speed and measured electrical power. The second loop is activated when the grid frequency exceeds predetermined limits. When the system frequency decreases, the reference torque is increased, allowing for the rotor to decrease speed and distribute the kinetic energy. DFIG utilizes its kinetic energy in response to frequency variations during load fluctuations. The active power supplied by the wind turbine amid any load fluctuations is ΔP_{NC}. The power supplied is compared to the power reference $\Delta P_{NC\text{ref}}$ for maximum output power. This is achieved by maintaining the rotor reference speed at the point where maximum power is attained. Equation (3.1) can be used to calculate the mechanical power captured by the wind turbine.

$$P_{mech} = \left(\frac{\frac{1}{2}(\rho A r)}{S_n} C_{p.opt} \right) \omega_s^3 \qquad 3.1$$

3.5 Modelling of TCPS

Figure (3.5) is a schematic of a two-area interconnected power system with a TCPS installed close to area one in series with the tie-line.

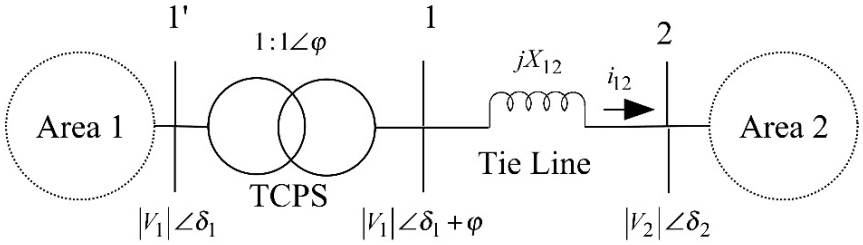

Figure 3.5: Model of a two-area interconnected power system with TCPS in series with tie-line [74].

Assuming the line losses to be negligible, the following derivation can be used to represent the TCPS model [74]:

The tie-line power flow between area one and area two can be expressed as:

$$\Delta P_{tie12}^{0}(s)=\frac{T_{12}}{s}\left[\Delta\omega_1(s)-\Delta\omega_2(s)\right] \tag{3.2}$$

The TCPS is installed close to area one, the current flow from area one to area two can be written as:

$$i_{12}=\frac{|V_1|\angle(\delta_1+\varphi)-|V_2|\angle(\delta_2)}{jX_{12}} \tag{3.3}$$

$$P_{tie12}-jQ_{tie12}=V_1^{*}i_{12}=|V_1|\angle-(\delta_1+\varphi)\left[\frac{|V_1|\angle(\delta_1+\varphi)-|V_2|\angle(\delta_2)}{jX_{12}}\right] \tag{3.4}$$

$$P_{tie12}-jQ_{tie12}=\frac{|V_1||V_2|}{X_{12}}\sin(\delta_1-\delta_2+\varphi)-j\frac{\left[|V_1|^2-|V_1||V_2|\cos(\delta_1-\delta_2+\varphi)\right]}{X_{12}} \tag{3.5}$$

Splitting the real parts of equation (3.5), results in;

$$\Delta P_{tie12}=\frac{|V_1||V_2|}{X_{12}}\cos\left(\delta_1^{o}-\delta_2^{o}+\varphi^{o}\right)\sin(\Delta\delta_1-\Delta\delta_2+\Delta\varphi) \tag{3.6}$$

Separating, δ_1, δ_2 and φ from their nominal value, $\delta°_1$, $\delta°_2$ and φ° in equation (3.6), produces:

$$\Delta P_{tie12}=\frac{|V_1||V_2|}{X_{12}}\cos\left(\delta_1^{o}-\delta_2^{o}+\varphi^{o}\right)\sin(\Delta\delta_1-\Delta\delta_2+\Delta\varphi) \tag{3.7}$$

$(\Delta\delta_1 - \Delta\delta_2 + \Delta\varphi)$ is extremely small so there is a minimal change in real power load, the bus voltage angles and TCPS phase angle variations are minimal and can therefore be written as:

$$\sin(\Delta\delta_1-\Delta\delta_2+\Delta\varphi)\approx(\Delta\delta_1-\Delta\delta_2+\Delta\varphi)$$

Hence,

$$\Delta P_{tie12}=\frac{|V_1||V_2|}{X_{12}}\cos\left(\delta_1^{o}-\delta_2^{o}+\varphi^{o}\right)(\Delta\delta_1-\Delta\delta_2+\Delta\varphi) \tag{3.8}$$

Let

$$T_{12} = \frac{|V_1||V_2|}{X_{12}} \cos\left(\delta_1^o - \delta_2^o + \varphi^o\right) \quad 3.9$$

So equation (3.8) may be reduced to:

$$\Delta P_{tie12} = T_{12}\left(\Delta\delta_1 - \Delta\delta_2 + \Delta\varphi\right) \quad 3.10$$

$$\Delta P_{tie12} = T_{12}\left(\Delta\delta_1 - \Delta\delta_2\right) + T_{12}\Delta\varphi \quad 3.11$$

Where

$$\Delta\delta_1 = \int \Delta\omega_1 dt \quad \text{and} \quad \Delta\delta_2 = \int \Delta\omega_2 dt \quad 3.12$$

From equation (3.11) and (3.12), results in:

$$\Delta P_{tie12} = T_{12}\left(\int \Delta\omega_1 dt - \int \Delta\omega_2 dt\right) + T_{12}\Delta\varphi \quad 3.13$$

The Laplace transformation of equation (4.13):

$$\Delta P_{tie12}(s) = \frac{T_{12}}{s}\left[\Delta\omega_1(s) - \Delta\omega_2(s)\right] + T_{12}\Delta\varphi(s) \quad 3.14$$

From equation (3.14), by controlling the phase shifter angle $\Delta\varphi(s)$ and the phase shifter angle $\Delta\varphi(s)$ can be represented as:

$$\Delta\varphi(s) = \frac{K_\varphi}{1 + sT_{PS}} \Delta Error(s) \quad 3.15$$

Hence, equation (3.14) may be rewritten as:

$$\Delta P_{tie12}(s) = \frac{T_{12}}{s}\left[\Delta\omega_1(s) - \Delta\omega_2(s)\right] + T_{12}\frac{K_\varphi}{1 + sT_{PS}} \Delta Error(s) \quad 3.16$$

It is assumed that the speed deviation $\Delta\omega_1$ is known and is therefore used as the control signal to the TCPS in order to control the TCPS phase angle, which controls the tie-line power flow. Therefore:

$$\Delta\varphi(s) = \frac{K_\varphi}{1 + sT_{PS}} \Delta\omega_1(s) \quad 3.17$$

And the tie-line power flow fluctuation becomes:

$$\Delta P_{tie12}(s) = \frac{T_{12}}{s}\left[\Delta\omega_1(s) - \Delta\omega_2(s)\right] + T_{12}\frac{K_\varphi}{1+sT_{PS}}\Delta\omega_1(s) \quad 3.18$$

$$\Delta P_{tie12}(s) = \Delta P^{o}_{tie12} + \Delta P_{TCPS}(s) \quad 3.19$$

Where

$$\Delta P_{TCPS}(s) = T_{12}\frac{K_\varphi}{1+sT_{PS}}\Delta\omega_1(s) \quad 3.20$$

The structure of TCPS as frequency regulator is shown in figure (3.6)

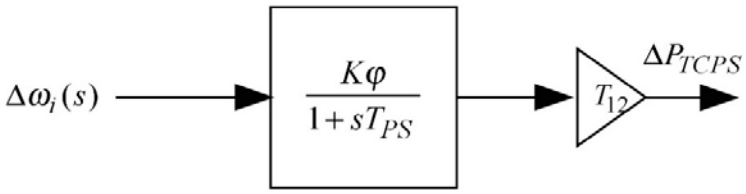

Figure 3.6: Transfer function of the TCPS.

3.6 Modelling of a SMES Unit

The schematic configuration of a SMES unit is shown in figure (3.7).

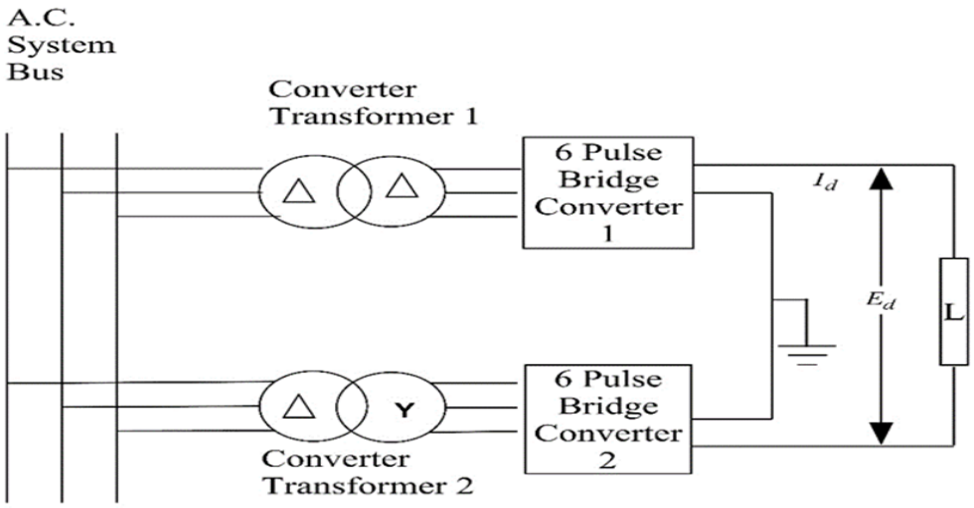

Figure 3.7: Schematic diagram of SMES unit [42].

The SMES unit contains a DC superconducting coil and converter which is connected to the grid by a Y-Δ/Y-Y transformer. By controlling the firing angle of the converter, a constantly changing DC voltage E_d is provided across the inductor within a certain range of positive and negative values. By applying a little positive voltage across the inductor, it is initially charged to its rated current $I_{do.}$ When the current reaches the rated value, it is maintained by decreasing the voltage across the inductor to zero as the coil is superconducting. In [80], the converter losses and the transformer losses are assumed to be zero and the DC voltage is given as:

$$E_d = 2V_{do}\cos\alpha - 2I_d R_c \qquad 3.21$$

Where,

E_d is the DC voltage applied to the inductor (kV);

V_{do} is the maximum circuit voltage (kV);

I_d is the current flowing through the inductor (kA);

α is the firing angle (º) and

R_c represents the equivalent commuting resistance (Ω).

If *α* is less than 90º, the converter will respond in charging mode and if *α* is greater than 90º, the converter will respond in discharging mode. In LFC, the DC voltage E_d across the superconducting inductor is constantly controlled depending on the ACE. The inductor voltage deviation of the SMES is based on ACE of the area in which it is located. The inductor current variation is employed as a feedback signal in the SMES loop. The feedback signal delivers a rapid restoration current when the load demand suddenly changes. After a sudden load fluctuation, the inductor current needs be restored to its nominal value rapidly so that it may respond to next load fluctuation [37].

The governing equations of the current deviation and the inductor voltage for each area in Laplace form is written as [42]:

$$\Delta I_{di}(s) = \frac{1}{sL_i}\Delta E_{di}(s) \qquad 3.22$$

$$\Delta E_{di}(s) = K_{0i}\frac{1}{1+sT_{dci}}\left[B_i\Delta f_i(s)+\Delta P_i(s)\right]-K_{Idi}\frac{1}{1+sT_{dci}}\Delta I_{di}(s) \quad 3.23$$

Where K_{Idi} is the feedback gain = ΔI_{di},

$K_{0\mathrm{i}}$ is the gain constant (kV/unit ACE);

L_{i} is the inductance of coil (H) and

T_{dci} represents the converter time delay.

The real power deviation in inductor of SMES unit can be written as:

$$\Delta P_{smi}(t) = \Delta E_{di} I_{di0} + \Delta I_{di}\Delta E_{di} \quad 3.24$$

Expressed in time domain, the energy stored in the SMES unit at any instant can be written as:

$$W_{smi}(t) = \frac{L_i I_{di}^2}{2} \text{ (MJ)} \quad 3.25$$

Figure (3.8) shows the resulting transfer function of SMES unit.

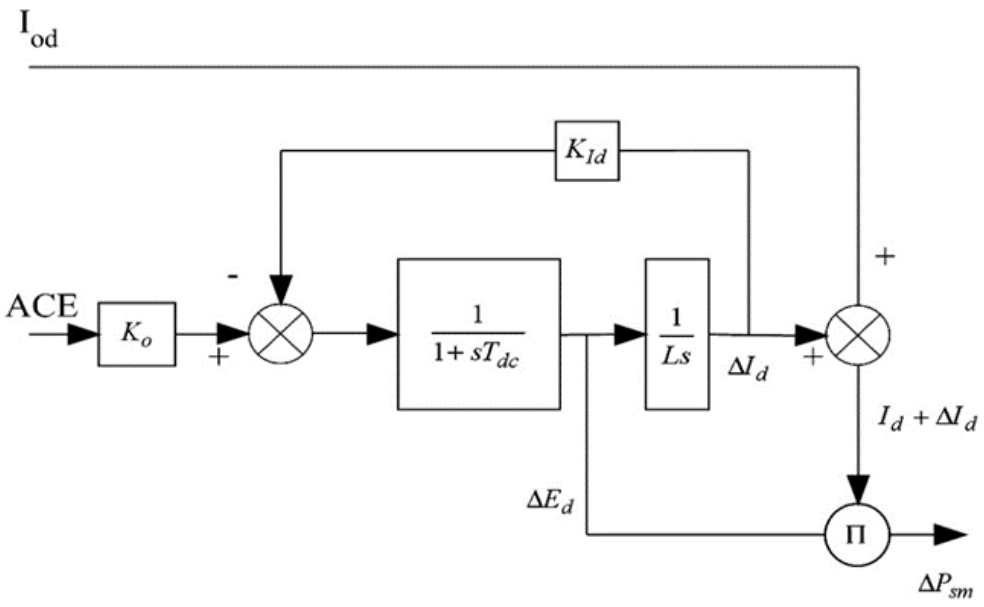

Figure 3.8: Transfer function of the SMES unit.

3.7 Modelling of the Optimal Controller

An s-area interconnected power system is represented by a direct time-invariant system within the state variable form [84]:

$$\frac{d}{dt}(X) = AX + BU + \Gamma P_d, \tag{3.26}$$

$$Y = CX \tag{3.27}$$

Where:

X represents the system parameter state;

U represents the control signal;

P_d represents the disturbance vector and

Y represents the system output.

A, B, C and Γ are the state, control, output and disturbance matrices respectively.

The control signal U minimises the performance index file J given by;

$$j = \int_0^\infty \frac{1}{2}\left[X^T QX + U^T RU \right] dt. \tag{3.28}$$

Within the implementation of an ideal control hypothesis, the term ΓP_{d} in equation (3.26) can be excluded by reclassifying the states in terms of their steady-state values after a load variation. Equation (3.26) can be adapted as follows:

$$\frac{d}{dt}\left(X \right) = AX + BU + \Gamma P_d, X\left(0\right) = X_0, \tag{3.29}$$

Equation (3.27) remains the same.

The full state vector control law is expressed in the form:

$$U^* = -\left[\Psi^* \right] X, \tag{3.30}$$

this reduces the performance execution function in equation (3.28).

The application of Pontryagin's Minimum Principle is applied reducing the network to its Riccati condition;

$$PA + A^T P - PBR^{-1}B^T P + Q = 0. \tag{3.31}$$

The arrangement of equation (3.30) produces a clear symmetric matrix *P*, and the ideal control law is represented by:

$$U^* = -R^{-1}B^T PX. \tag{3.32}$$

The optimal system matrix with complete feedback gain is;

$$\left[\psi^*\right] = R^{-1}B^T P. \tag{3.33}$$

3.8 System Vector for the Optimal Control Design

The structures of the three power system models given in figures (3.1 - 3.3) can be represented in its state variable form by equations (3.26) and (3.27). The structure of the vectors and matrices are defined by the transfer function model shown in figure (3.4). The structure for each model is as follows:

Model 1

State vector

$$\left[X_1\right]^T = \left[\int ACE_1 dt \;\; \Delta X_{E1} \;\; \Delta P_{M1} \;\; \Delta F_1 \;\; \Delta P_{tie12} \;\; \int ACE_2 dt \;\; \Delta X_{E2} \;\; \Delta P_{x1} \;\; \Delta P_{x2} \;\; \Delta P_{M2} \;\; \Delta F_2 \right],$$

Control vector

$$\left[U_1\right] = \begin{bmatrix} \Delta P_{C1} \\ \Delta P_{C2} \end{bmatrix},$$

Disturbance vector

$$\left[P_{d1}\right] = \begin{bmatrix} \Delta P_{d1} \\ \Delta P_{d2} \end{bmatrix}.$$

Model 2

State vector

$$[X_2]^T = \begin{bmatrix} \int ACE_1 dt\ \Delta X_{E1}\ \Delta P_{M1}\ \Delta F_1\ \Delta P_{tie12}\ \Delta X_{1-1}\ \Delta X_{2-1}\ \Delta X_{3-1}\ \Delta P_{NC1}\ \Delta\omega_1 \\ \int ACE_2 dt\ \Delta X_{E2}\ \Delta P_{x1}\ \Delta P_{x2}\ \Delta P_{M2}\ \Delta F_2\ \Delta X_{1-2}\ \Delta X_{2-2}\ \Delta X_{3-2}\ \Delta P_{NC2}\ \Delta\omega_2 \end{bmatrix},$$

Control vector

$$[U_2] = [U_1],$$

Disturbance vector

$$[P_{d2}] = [P_{d1}].$$

Model 3

State vector

$$[X_3]^T = \begin{bmatrix} \int ACE_1 dt\ \Delta X_{E1}\ \Delta P_{M1}\ \Delta F_1\ \Delta P_{tie12}\ \Delta X_{1-1}\ \Delta X_{2-1}\ \Delta X_{3-1}\ \Delta P_{NC1}\ \Delta\omega_1 \\ \int ACE_2 dt\ \Delta X_{E2}\ \Delta P_{x1}\ \Delta P_{x2}\ \Delta P_{M2}\ \Delta F_2\ \Delta X_{1-2}\ \Delta X_{2-2}\ \Delta X_{3-2}\ \Delta P_{NC2}\ \Delta\omega_2\ \Delta P_{TCPS}\ \Delta P_{SMES} \end{bmatrix},$$

Control vector

$$[U_2] = [U_1],$$

Disturbance vector

$$[P_{d2}] = [P_{d1}].$$

The system state, control and disturbance matrices are provided in appendix D.

3.9 Simulation Results and Analysis

The optimal LFC strategy was based on performance index minimization through full state vector feedback using an ACE controller. The controller was designed for a two-area interconnected power system with active support from DFIG based wind turbines in each area as illustrated in figures (3.1 - 3.2). In area one, hydro

power is generated and in area two the power is generated through thermal turbines. The two areas are linked via AC tie-lines. In addition to the support of wind generations with DFIG based turbines in each area, the effectiveness of a TCPS in series to the AC tie-line and a SMES unit installed in area two as shown in figure (3.3), was also investigated. The optimal control strategy was developed by considering system state parameters for the three power system models under investigation. The LFC strategy was analysed to determine its effectiveness in restoring optimum system frequencies and maintaining tie-line power stability after sudden load fluctuations.

The controller was simulated in MATLAB/Simulink 2019 and the outputs of the control action were analysed on the basis of performance index minimization values, closed ring eigenvalues, controller feedback gains and the graphical results obtained from the simulations. The analysis were done on the basis of 1 % load demand increase in the hydro power generating system (area one). Further analysis were done with 1 % load demand increase in the hydro generating system (area one) and 2 % load demand increase in the thermal system (area two). The analysis was done through the simulated results in tables (3.1 – 3.3) and the graphical results in figures (3.9a-d) and figures (3.10a-d).

The data in table (3.1) displays the Performance Index (PI) values for the three power system models. The PI values indicates the error in the system during load fluctuations.

Table 3. 1: Optimum PI values for the three developed models.

Optimal FC	**Optimal FC + DFIG**	**Optimal FC+ DFIG+TCPS-SMES**
13.1619	1.1668	1.0203

The greater the error value implies greater variations in system state parameters implying poor performance of the control action. Theoretically, this value should return to zero implying that optimum operating conditions have been restored and there are no system parameter variations. However due to the mechanical

components in the system, which has long settling times, the effectiveness of the control strategy is determined by the PI values being close to zero. During the simulated 1 % load fluctuation, using only the optimal controller, the system error was high as indicated by the high PI value of 13.1619.

When the control strategy was supported with the integration of wind power generation in each area using DFIG based wind turbines, the PI value was reduced from 13.1619 to 1.1668. This was a significant reduction in the PI value, which demonstrated that the injection of kinetic energy into the system from the DFIG based wind turbines, significantly improves the dynamic performance of the system during load fluctuations.

The PI value was further reduced from 1.1668 to 1.0203 when the TCPS is linked in series to the AC tie-line with a SMES unit installed in area two of the interconnected system. Although the error value was further reduced with the implementation of the FACTS devices, the reduction was not as huge as expected. This indicated that the SMES unit installed in area two did not have a significant control impact to load fluctuations in area one.

The feedback gains for each state for the three power system models are shown in table (3.2). The feedback gains indicate the effectiveness of the control action. From the analysis, it was observed that there were substantial increases in the feedback gains of the optimal controller with the kinetic inertial support provided by the DFIG based wind turbines. Further increase in the feedback gains were observed with the inclusion of the TCPS in series with the tie-line and a SMES unit installed in area two of the interconnected power system.

Table 3.2: Feedback gains for each state of the three developed models.

Optimal FC	
Area 1	[0.9889 2.0820 0.2825 1.2375 -0.0644 0.1483 0.0375 -0.0788 0.4989 0.3715 -0.0300;
Area 2	-0.1483 0.1046 0.0448 0.1794 1.4592 0.9889 0.732 0.0267 2.1291 1.5838 0.5870]
Optimal FC + DFIG	
Area 1	[0.9963 2.2476 0.3360 1.3053 -0.8969 0.4171 -0.639 -1.7431 1.3925 -2.9097 0.0863 -0.0034 -0.0281 0.233 0.0484 -0.0915 0.1691 -0.1648 -0.5303 -0.0703 -0.8312
Area 2	-0.0863 0.0684 0.0312 0.1315 1.3494 0.0041 -0.011 -0.1275 0.0649 -0.1863 0.9963 0.6901 0.0014 1.682 1.6579 0.5722 0.9308 -1.0779 -2.8589 0.8328 -5.0095]
Optimal FC+DFIG +TCPS-SMES	
Area 1	[0.9919 2.4661 0.4109 1.4889 -1.2684 0.4321 -0.682 -1.8396 1.5936 -3.0604 0.1270 0.0194 -0.0388 0.153 0.2225 0.0464 0.0940 -0.1181 -0.4178 0.0853 -0.6638 0.034 -0.0070;
Area 2	-0.1270 0.0879 0.0374 0.1445 0.6438 0.0142 -0.0253 -0.1445 0.0865 -0.2078 0.9919 0.6562 0.0393 1.5926 1.3274 0.4150 0.8594 -0.9660 -2.5817 0.6251 -4.5781 -0.0402 -0.0875]

The closed loop eigenvalues of the three power system models are shown in table (3.3).

Table 3.3: Eigenvalues analysis for the three developed models.

Optimal FC	**Optimal FC + DFIG**	**Optimal FC+ DFIG+TCPS SMES**
-35.4798 + 0.0000i	-35.5300 + 0.0000i	-35.5709 + 0.0000i
-11.1466 + 0.0000i	-11.1796 + 1.7455i	-32.5896 + 0.0000i
-6.1515 + 0.9164i	-11.1796 - 1.7455i	-11.7485 + 0.0000i
-6.1515 - 0.9164i	-11.6357 + 0.0000i	-10.1995 + 1.8141i
-3.3127 + 0.0000i	-6.4103 + 1.4819i	-10.1995 - 1.8141i
-1.0758 + 2.3560i	-6.4103 - 1.4819i	-5.6829 + 4.0859i
-1.0758 - 2.3560i	-4.2347 + 3.7554i	-5.6829 - 4.0859i
-2.4821 + 0.0000i	-4.2347 - 3.7554i	-6.4152 + 1.4772i
-0.4061 + 0.0000i	-1.6916 + 3.8277i	-6.4152 - 1.4772i
-0.3059 + 0.1820i	-1.6916 - 3.8277i	-10.0000 + 0.0000i
-0.3059 - 0.1820i	-2.4382 + 0.0000i	-1.9851 + 4.0339i
	-1.0812 + 0.0000i	-1.9851 - 4.0339i
	-0.4888 + 0.3019i	-2.4499 + 0.0000i
	-0.4888 - 0.3019i	-0.7673 + 0.0000i
	-0.4137 + 0.0000i	-0.4969 + 0.3241i
	-0.2287 + 0.0000i	-0.4969 - 0.3241i
	-0.1862 + 0.0281i	-0.4397 + 0.0000i
	-0.1862 - 0.0281i	-0.2093 + 0.0000i
	-0.1667 + 0.0000i	-0.1776 + 0.0341i
	-0.1000 + 0.0000i	-0.1776 - 0.0341i
	-0.1000 + 0.0000i	-0.1668 + 0.0000i
		-0.1000 + 0.0000i
		-0.1000 + 0.0000i

The review of the closed loop real and imaginary components of the eigenvalues demonstrated that the closed loop power system stability was guaranteed for all system state scenarios. The eigenvalues indicated that the real and imaginary components of the system increased progressively when the DFIG based wind turbines were installed in each area of the power system. This demonstrated the positive impact of wind integrations in each area using DFIG based wind turbines. Further progression was achieved in the real and imaginary components of eigenvalues when dynamics of TCPS and SMES were considered in conjunction with DFIG in the interconnected hydro-thermal power system. This indicated that

installing the FACTS devices as part of the control strategy enhanced the dynamic performance of the system, during sudden load fluctuations

The parameter variations and response times, for the frequency in each area, the tie-line power and the area control error, for 1 % load increase in the hydro plant (area one) are shown in figures (3.9a-d).

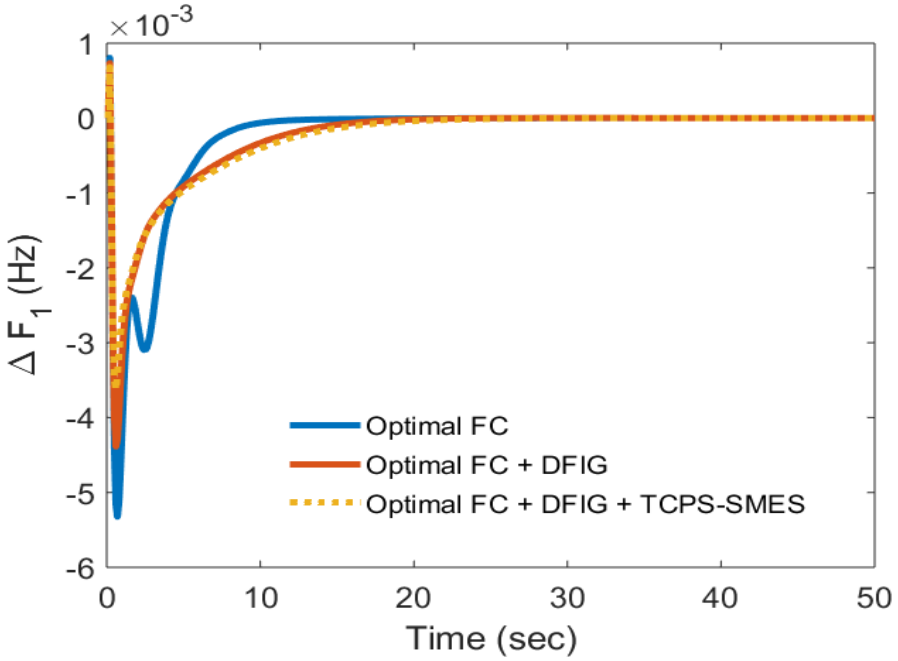

Figure 3.9a: Frequency response in area one for 1 % load increase in the hydro plant

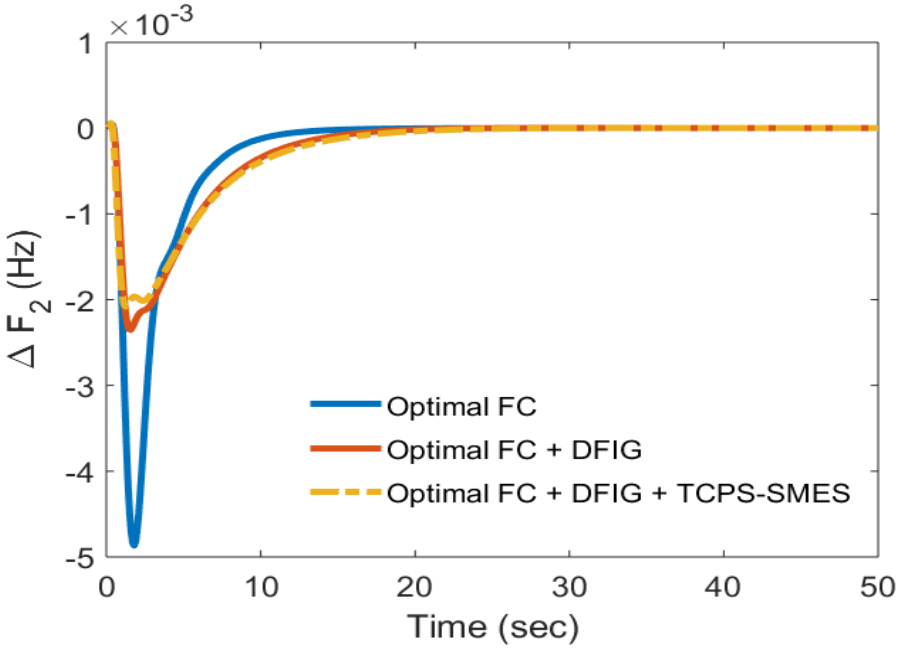

Figure 3.9b: Frequency response in area two for 1 % load increase in the hydro plant

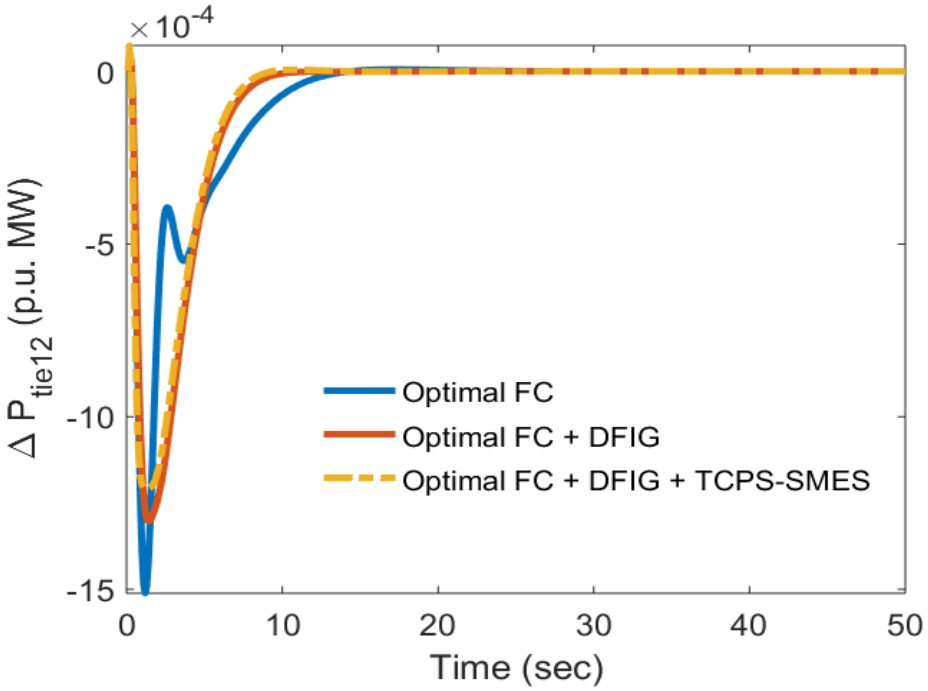

Figure 3.9c: Tie-line power response for 1 % load increase in the hydro plant

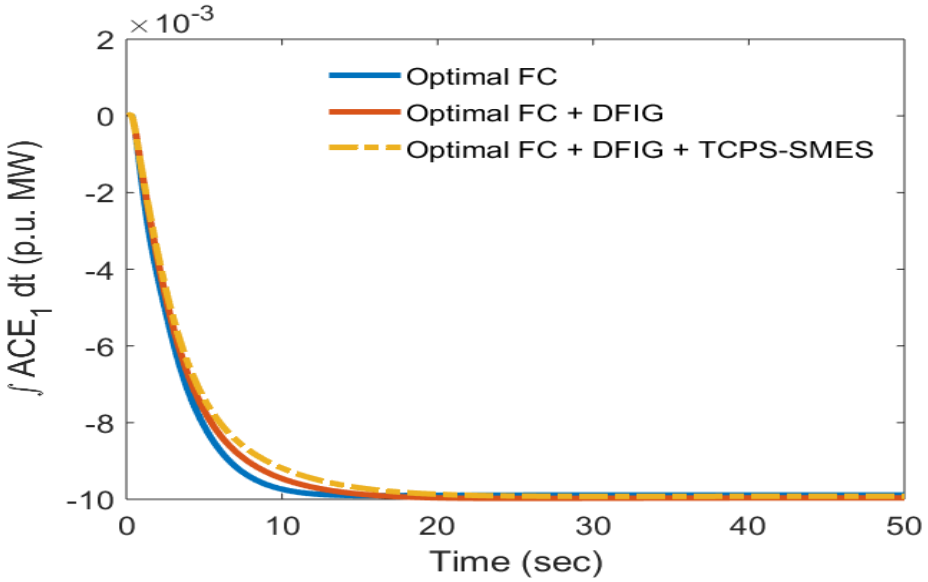

Figure 3.9d: Area control error for 1 % load increase in the hydro plant

In figures (3.9a-b) it was observed that the frequency variations in both areas were comparatively large with only the optimal control action. With the active contribution of the DFIG based wind turbines and the support of the TCPS-SMES, the frequency variations progressively reduced in area one but in area two there was a quick and drastic reduction. From figure (3.9c) it was observed that, with

the active participation of the DFIG based wind turbines and the TCPS-SMES, the tie-line power deviation is reduced, with a smoother restoration curve and faster settling times and the area control error was also reduced.

The parameter variations and response times, for the frequency in each area, the tie-line power and the area control error, for 1 % load increase in area one and 2 % load increase in area two are shown in figures (3.10a-d).

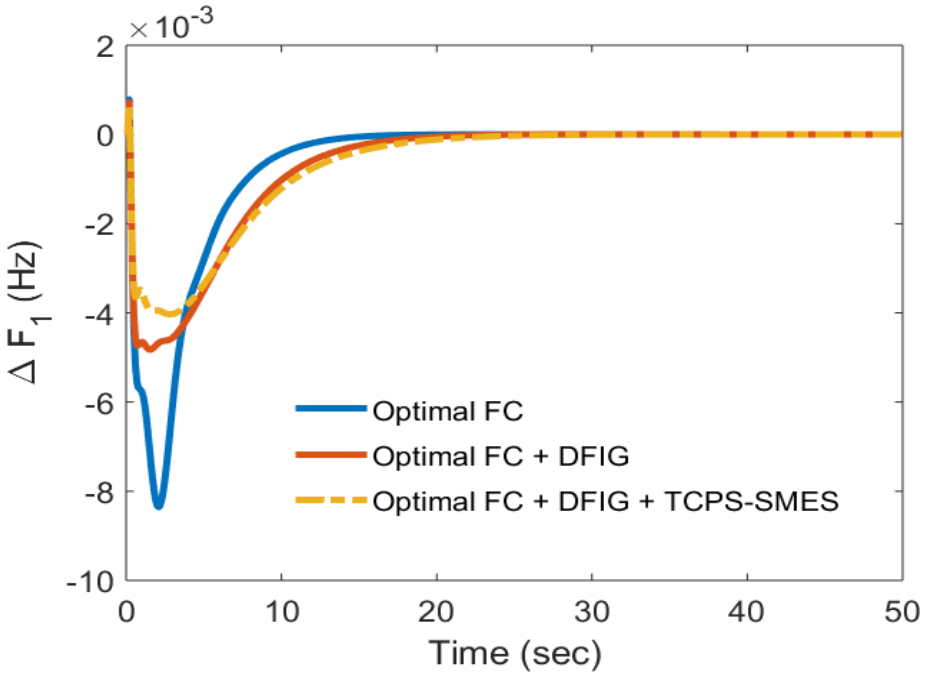

Figure 3.10a: Frequency response in area one for 2 % load increase in area two

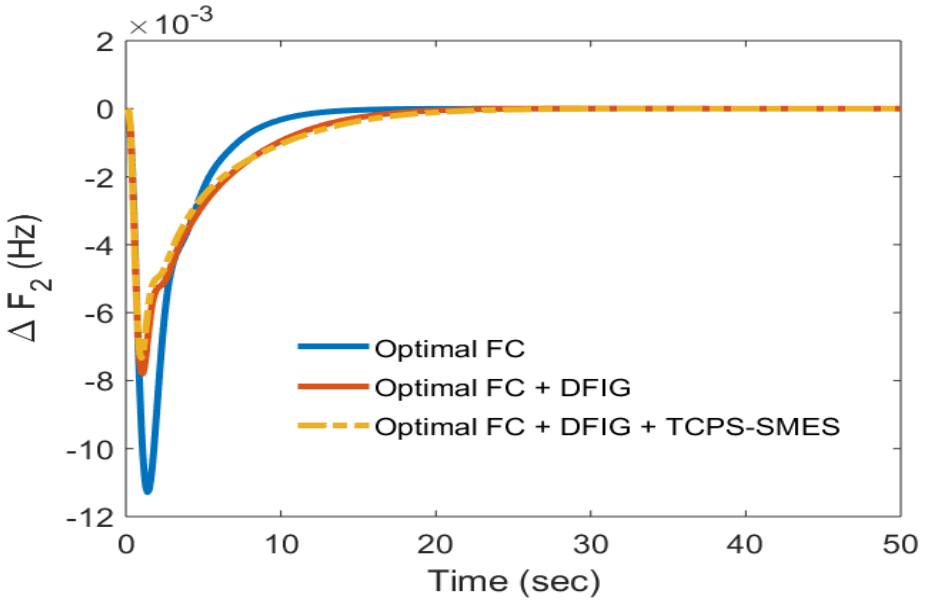

Figure 3.10b: Frequency response in area two for 2 % load increase in area two

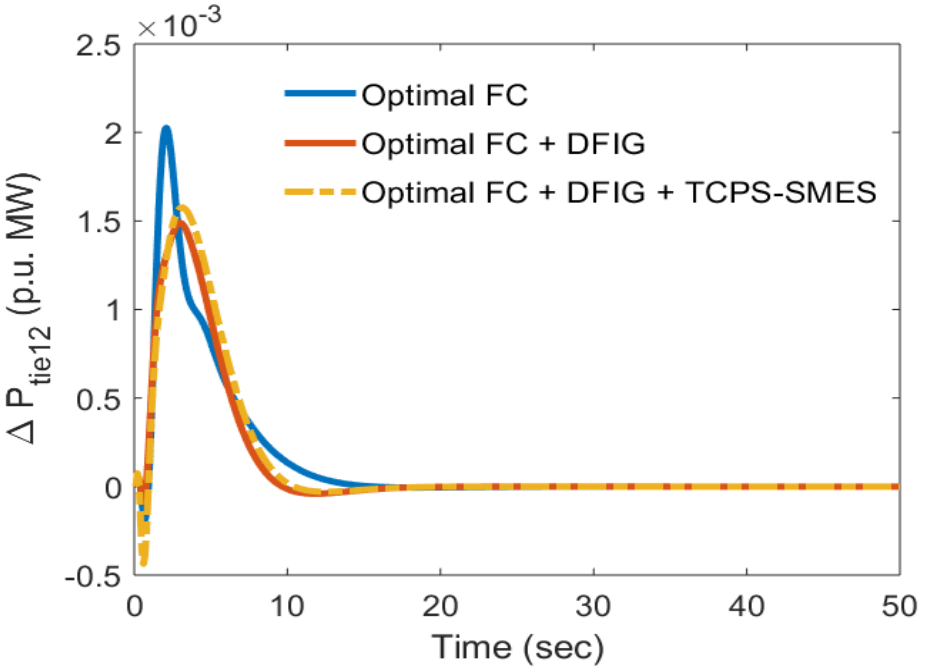

Figure 3.10c: Tie-line power response for 2 % load increase in area two

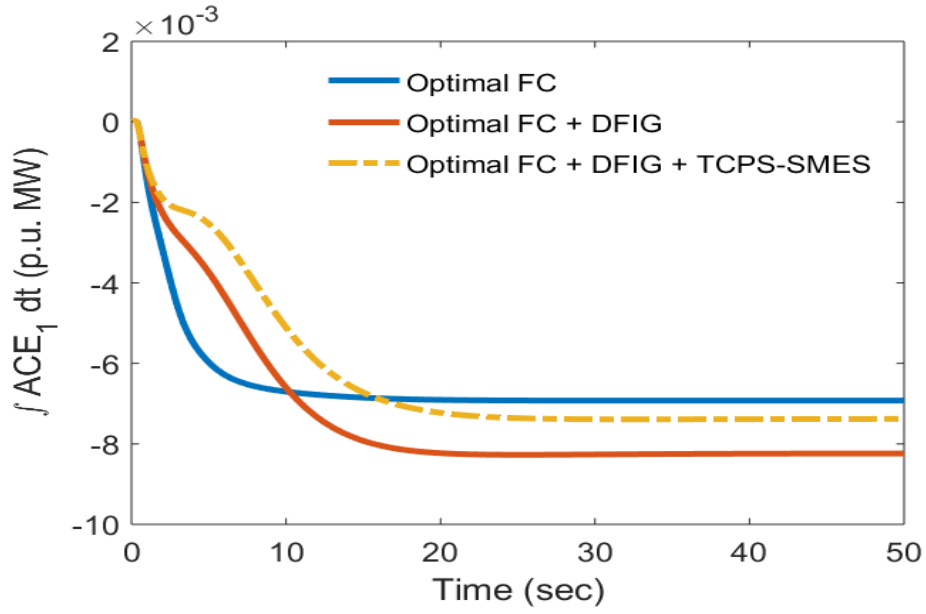

Figure 3.10d: Area control response for 2 % load increase in area two

From figures (3.10a-d) it was observed that the area frequencies and tie-line power variations are greater compared to those observed in figures (3-9a-d), which was expected due to the additional load increase in area two. However these graphs demonstrated the power system's dynamic performance is enhanced with the support of the DFIG based turbines and the TCPS-SMES.

3.10 Discussion

This chapter presented the design and simulation of an optimal LFC strategy. The design was based, on error minimisation through full state vector feedback, using an ACE controller, for a two area interconnected power system consisting of hydro generation in area one and non-reheat thermal turbines in area two (model one). The analysis and simulation were done with the active participation of DFIG based wind turbines in each area (model 2) and the dynamic support of TCPS-SMES (model 3).

The results obtained in tables (3.1--3.3) demonstrated the positive impact of the optimal control strategy in achieving frequency and tie-line power stability for sudden load disturbances in the power system. The PI values (table 3.1) were reduced from 13.1619 to 1.1668 with the intergration of wind genearations employing DFIG based wind turbines in each area. The feedback gains (table 3.2) increased after DFIG based turbines were incorporated in each area. Finally the eigenvalues (table 3.3) showed that the real and imaginary component values of the system also increased with the installation of DFIG in each area. The output of the optimal controller was enhanced, with power intergrations in each area with the DFIG based wind turbines, that provided inertial support in each area. This clearly demonstrated the positive impact of DFIG based wind power integration in each area of the interconnected power system. Further improvements were achieved in model three of the system. With the DFIG based wind turbines providing inertial support in each area, a TCPS was installed in series with the tie-line and a SMES unit was installed in area two. The PI value were further reduced to 1.0203. The feedback gains and the real and imaginary components of the eigenvalues increased progressively. This guaranteed the steady state and dynamic output for optimal LFC for the interconnected power system in restoring system frequency and tie-line power stability after sudden load fluctuations.

The comparative responses for frequency variations and tie-line power, for each power system model under investigation were presented in figures (3.9a-d) and

figures (3.10a-d). These graphs clearly verified that wind power integration with DFIG based wind turbines have the ability to store excessive generated power from the rotor of the generators when there is excessive power available in the system. This excessive power can immediately contribute to the interconnected power system when the load demand exceeds the generation capacity. This allows for the system to reach optimum system frequency with reduced overshoot and faster response times by managing the generated power to compensate for varying load requirements. Also, it was observed that the DFIG in conjunction with the pair of TCPS-SMES improves the capability of the controller to restore the optimal frequency of the system with a lower first peak, oscillation free system results and faster steady state performance of the interconnect power system.

3.11 Conclusion

The results obtained in this chapter are positive but optimal control strategies based on full state vector feedback, requires all the state variables to be known. This is virtually impossible to achieve in a real power system. Also, the rated system parameters may not necessary be the true (real) system parameters due to general ‘wear and tear’ and environmental factors. This is especially true for the mechanical (moving) components in a power system. These associated problems can be eliminated and the controller may have a realistic chance of being practically implemented, by employing an optimal control strategy design, based on easily measurable outputs. The next chapter presents an optimal control strategy based on a MPC concept that requires only few state parameters that can be readily obtained as system outputs.

Chapter 4: Model Predictive Control

4.1 Introduction

It was demonstrated in chapter three that power system stability can be significantly enhanced with optimal control strategies. However, an optimal control design, based on a full state feedback control law, which is a function of all the system state parameters, are not practically feasible. Generally, it is not possible to obtain all system state parameters, therefore the feasibility of implementing these control strategies in practical situations is a difficult challenge for power engineers to overcome.

A basic prerequisite for an effective control strategy is a precise mathematical model but it is extremely problematic to model a large, complex interconnected power system accurately. Many system state parameters are unattainable and numerous assumptions are made in the design process which would adversely affect the control strategy. Subsequently, this chapter presents the design of an optimal LFC strategy based on a model predictive control (MPC) concept, for a two-area interconnected power system. The MPC strategy is relative simple in design and implementation compared to control strategies based on full state vector feedback and the MPC provides superior control action compared to a control strategy based on classical control theory. The MPC strategy relies on output vector feedback and only requires two system state parameters; system frequencies and tie-line power flow which are easily assessable as outputs.

4.2 Review of the Model Predictive Control Strategy

Various methods have been proposed to deal with the difficulties associated with implementing control strategies based on full state vector feedback., The decentralised dual-mode [81], changing structure model [82] and optimal structure design [83], are few examples, but these proposed models are so complex that they did not gain any traction. Techniques based on system state reconstruction could be employed to overcome this problem but this is also very

complex in design. The concept of sub-optimal LFC design were introduced to avoid the problems related to optimal controllers [84], however, a controller design based on sub-optimal control only works well in the case of true system parameters but does not guarantee to provide the desired performance in the case of parameter variations of the power system equipment. True (actual) system parameters may not be the rated system parameters because of the general 'wear and tear' of system components over time. Several control strategies based or artificial intelligence and intelligent techniques have been proposed [76]. These techniques will have a profound influence in power system designs in the future, however, at present it is unrealistic that any new power system being developed now, will employ such techniques.

Alternatively, an optimal control strategy, employing the MPC concept is an effective control strategy for its potential applications in industry. MPC is a control algorithm constructed on a power system model, utilising an optimization performance procedure in every sampling interval to determine a future optimal control action. It is decisively functional because it can handle constraints on the control as well as system states and output variables. A MPC strategy is proposed in [85], with the support of DFIG based wind turbines. The analysis demonstrated that system stability was guaranteed by employing an independent MPC in each control area. In [86], the MPC included the modelling of dynamic valve positioning for a hydro-thermal plant. The simulated results showed the rapid response times to system frequency variations. A MPC design including the support of DFIG based wind turbines is investigated in [87], comparisons were done with and without the support of DFIG. The results demonstrated the positive impact of DFIG in the control strategy. The investigation in [88] validated the robustness of the MPC by taking into account the GRC constraints.

The advantage of the MPC is its relative simplicity in design and the implementation of the control action. The MPC only requires two system state parameters; the frequency in each area and the tie-line power variations. These parameters are easily assessable as system outputs. The frequency and tie-line

power variations are combined to obtain an area control error. The control error reference is set to zero, meaning no system variations. The continuously changing system states results in continuous system variations meaning continuous control errors. These are monitored against the error reference and the necessary control action is provided. When an identical error occurs the controller predicts the control action based on previous actions. The ability to incorporate economic objectives as part of the control requirements makes the MPC a viable candidate for practical LFC strategies. In view of the above discussion, this chapter subsequently presents the design, simulation and comparative analysis of a MPC based LFC regulator and a conventional integral controller, for a two-area interconnected power system consisting of thermal generations in each area.

4.3 Model under Study

A two-area interconnected power system consisting of thermal power plants having non-reheat turbines in each area, combined with DFIG based wind turbines in each area, a TCPS installed near area one in series with the tie-line and a SMES unit installed at the terminal of area two, is considered for the present investigations. The transfer function model of the power system is shown in figure (4.1). The transfer function models of the TCPS and the SMES unit were developed in chapter three.

4.4 Generation Rate Constraints Model

Most of the research in this area ignores the effects of the restriction on the rate of power generation (GRC) [80]. In steam plants, the power generation can only increase at a specified maximum rate owing to the physical limitations of the mechanical components in the system. If these constraints are ignored, the system would experience huge turbulences resulting in power system instability and possible system shutdown. Therefore, the GRC for the thermal power plant; for a range of ± 10%/min (0.0017pu/s) is considered in this investigation. Figure (4.2) is an illustration of the non-linear turbine model with GRC.

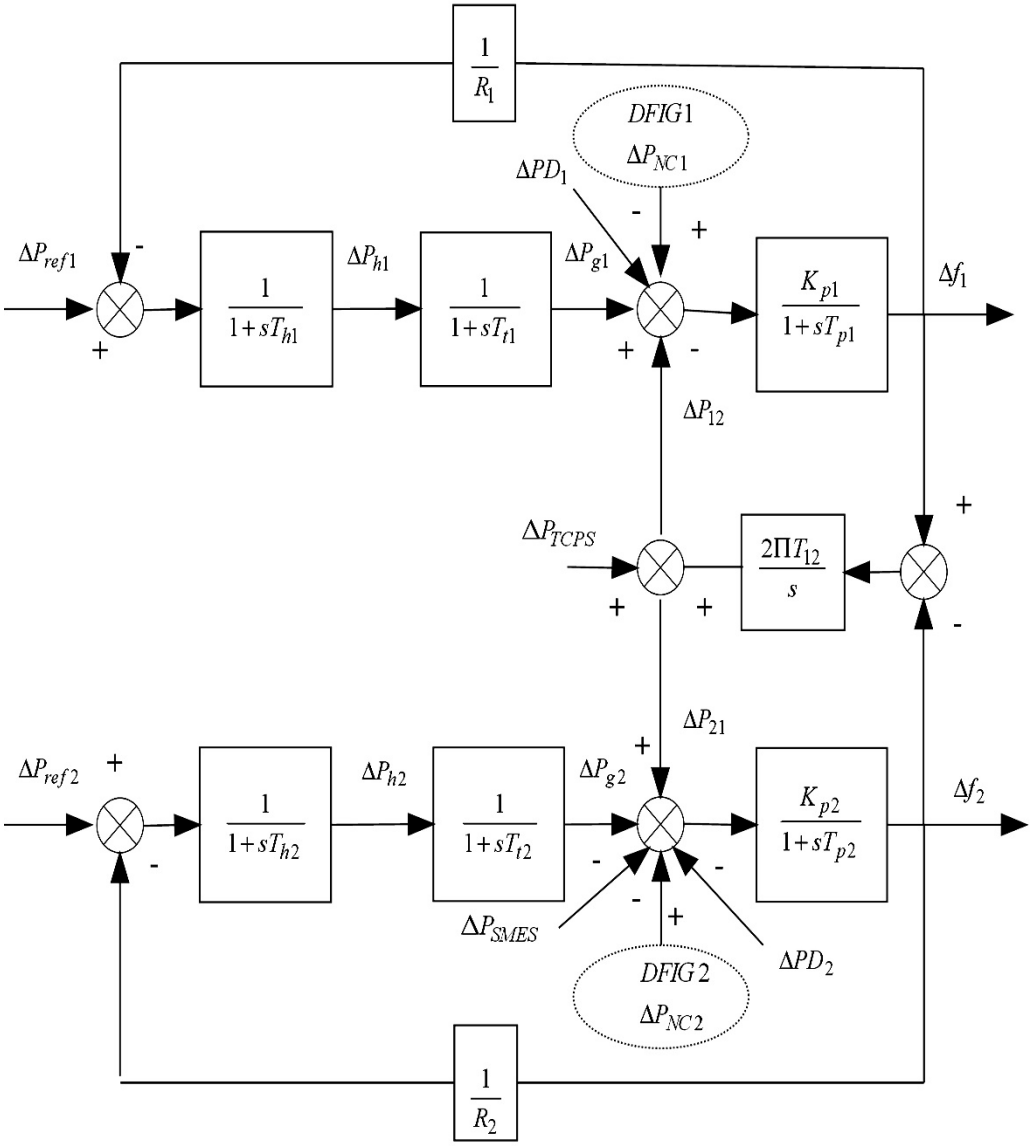

Figure 4.1: Transfer function model of a two-area interconnected power system with DFIG based wind turbines in coordination control of TCPS-SMES.

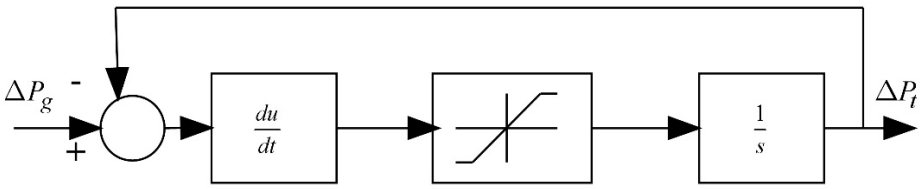

Figure 4.2: Non-linear turbine model with GRC

4.5 Model Predictive Control Design

The Model Predictive Control (MPC) is generally accepted as an effective control strategy in the design of various industrial control systems [85]. The MPC is constructed on an explicit use of a prediction model to obtain control actions for future control reactions by minimising the objective function. The optimisation objectives include the minimisation of the difference between the predicted reaction and reference dynamic response subjected to predetermined limitations. In the MPC regulator design, the first input in the optimal sequence is sent into the plant and the entire calculation is repeated at subsequent control intervals. The notion of obtaining new measurements at each time interval is to compensate for model inaccuracies and unexpected load disturbances, resulting in the system output being different from the one predicted by the model.

The internal model of the plant is developed to predict the future outputs based on the past and current values of the inputs and outputs of the power system. The total prediction in MPC design can be calculated by combining both the free and forced responses. The optimiser is used to calculate the best set of future control actions by minimising a cost function (J), subject to the constraints on both the manipulated and the control variables [85].

The cost function to be minimised is a combination of the square of the predicted errors and the square of the future control values is given as;

$$J\left(N_1, N_2, N_u\right) = \sum_{j=N_1}^{N_2} \beta(j)\left[\hat{y}(k+j\,|\,k) - w(k+j)\right]^2 + \sum_{j=1}^{N_u} \lambda(j)\left[u(k+j-1)\right]^2 \qquad 4.1$$

Where N_1 and N_2 *represent* the lower and upper prediction horizon over the output, N_u represents the control horizon, $\beta(j)$ and $\lambda(j)$ are weighting factors. According to the MPC technique, the control horizon reduces the number of calculated future controls according to the relation: $\Delta u\,(k+j)$ for $(j \geq N_u)$. The $w\,(k+j)$ is the reference trajectory over the future horizon N. The restrictions on the control signal, the outputs and the control signal change are added to the cost function as presented in [85]:

$$u_{\min} \le u(k) \le u_{\max}$$

$$\Delta u_{\min} \le \Delta u(k) \le \Delta u_{\max}$$

$$y_{\min} \le y(k) \le y_{\max} \qquad 4.2$$

The Solution for equation (4.1) stipulates the optimal sequence of the control signal over the horizon *N* subject to the restrictions of equation (4.2). Figure (4.3) is a simple schematic diagram of the MPC arrangement.

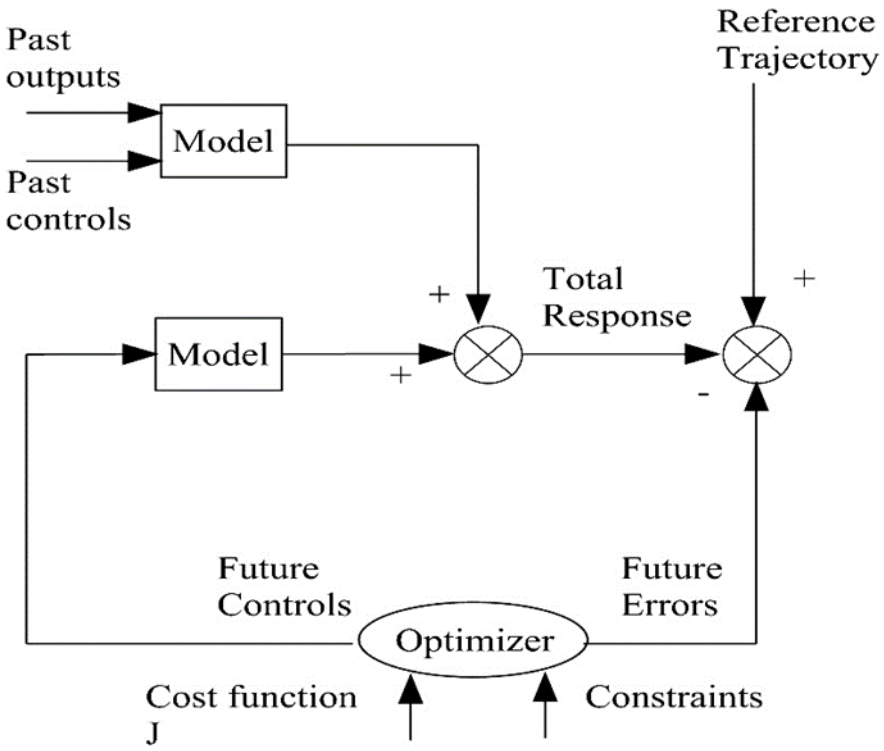

Figure 4.3: Simplified schematic diagram of MPC scheme.

4.6 Simulations Results and Discussion

During a sudden load change, the active power was injected from DFIG wind turbines with additional power support from a TCPS located in series with the tie-line and SMES unit installed in area two of the power system. The frequency variations in both areas, the tie-line power deviation and the area control error

responses of the interconnected power system were obtained by simulating the power system model with the MPC design for 1 % load fluctuation in area one. The results were compared to a conventional integral controller with the same system model and similar operating conditions. The system responses obtained are shown in Figures (4.4a-d)

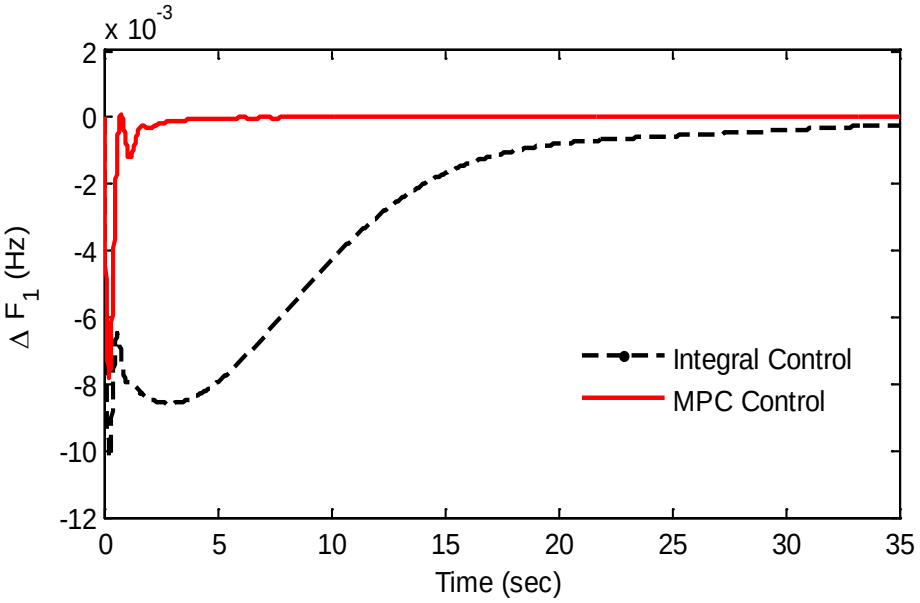

Figure 4.4a: Frequency response in area one for 1 % load fluctuation in area one.

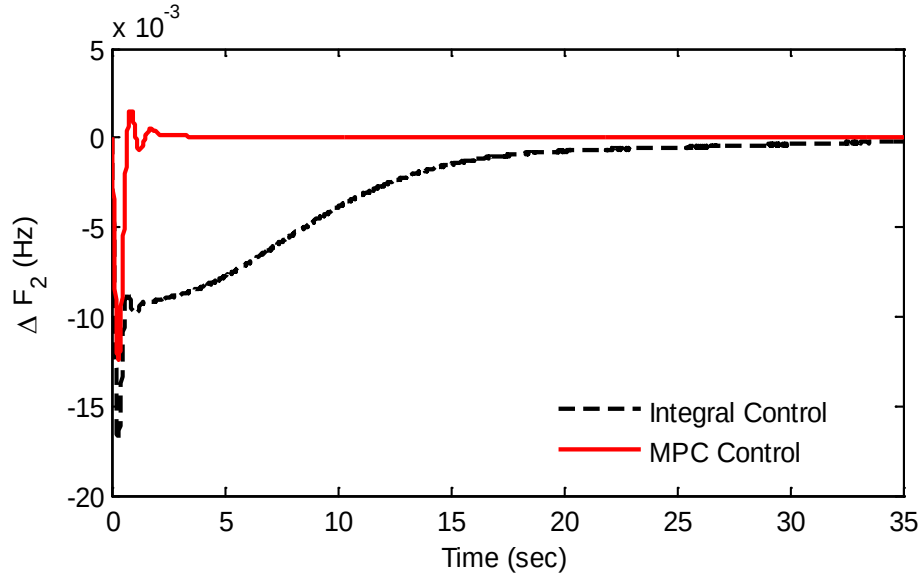

Figure 4.4b: Frequency response in area two for 1 % load fluctuation in area one.

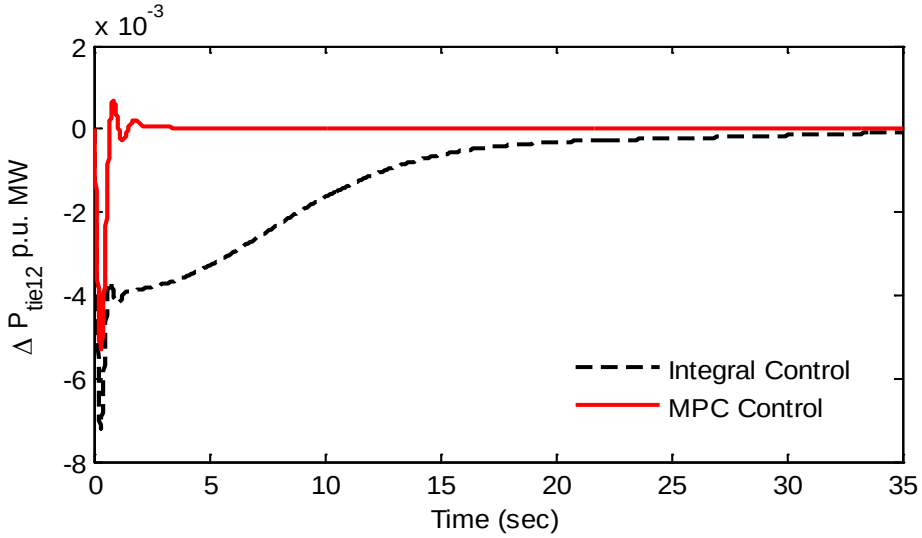

Figure 4.4c: Tie-line power response for 1 % load fluctuation in area one.

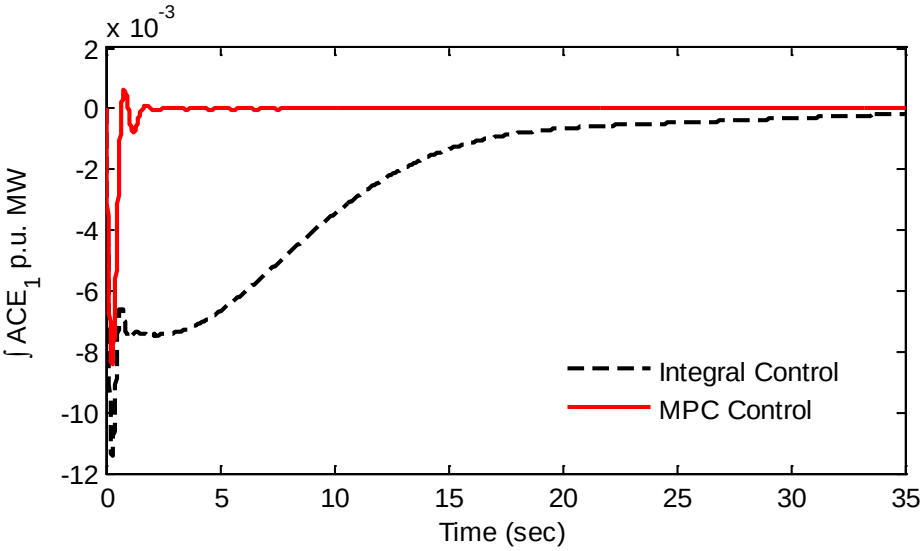

Figure 4.4d: Area control error for 1 % load fluctuation in area one.

It was observed from the graphs in figures (4.4a-d) that the MPC was fast enough to match the system load demand with the generated power. The various system time responses returned to zero within three seconds. The integral controller was unable to return to a zero steady state condition within thirty seconds. That is a significant performance difference between the two controllers. It was also observed that the first peak of an over shoot for the MPC was significantly less for various system responses in comparison to the integral controller.

An additional step was taken to verify the performance of the MPC by considering

the limit on the rate of change in the steam generating power plants in each area (the GRC in both areas), to avoid damage of power system components. The parameter responses obtained for 1 % load demand increase with GRC in both areas are shown in figures (4.5a-d). These figures also display the response of the MPC and integral control without considering GRC.

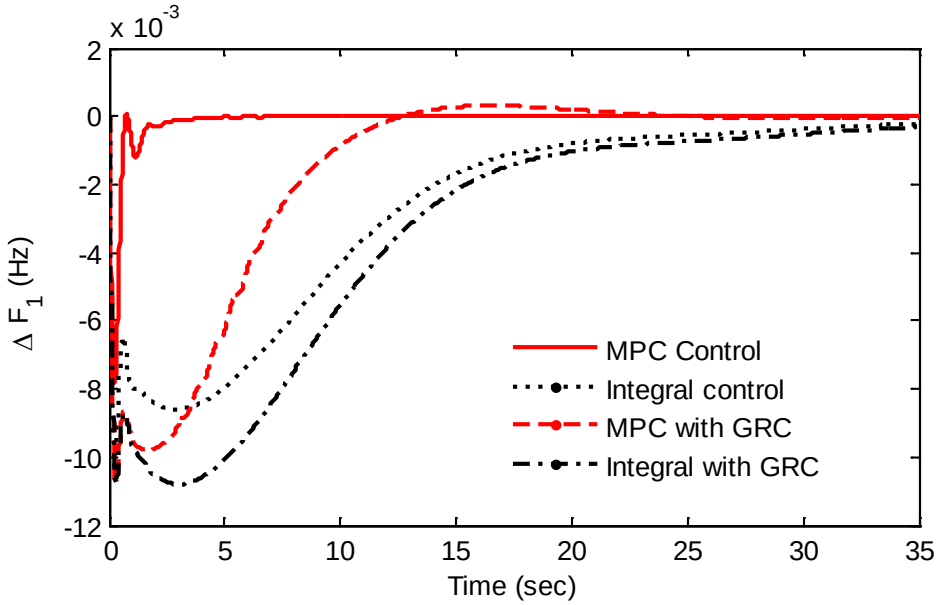

Figure 4.5a: Frequency response in area one for 1 % load demand increase with GRC in both areas.

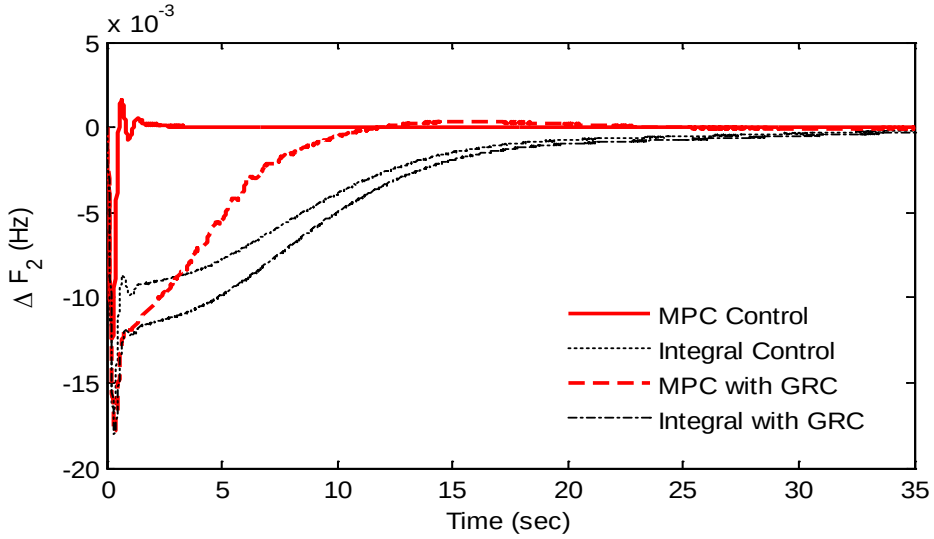

Figure 4.5b: Frequency response in area two for 1 % load demand increase with GRC in both areas.

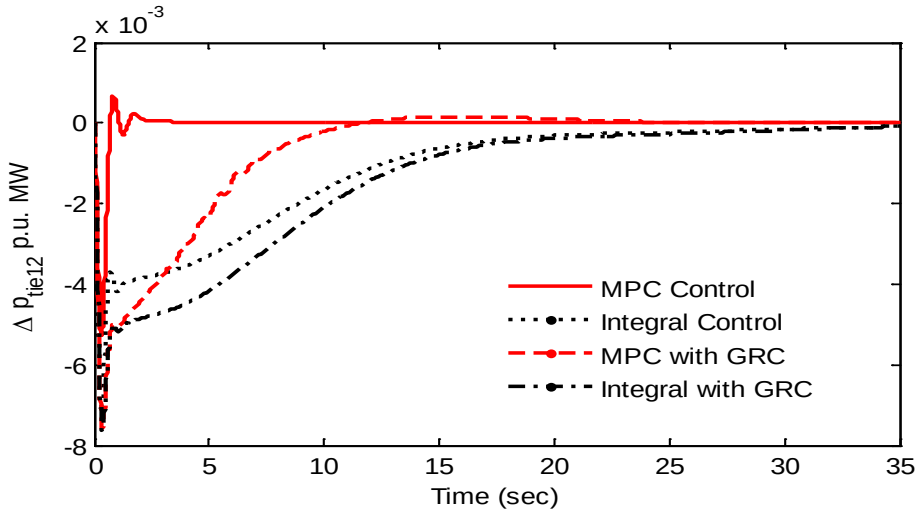

Figure 4.5c: Tie-line power response for 1 % load demand increase with GRC in both areas.

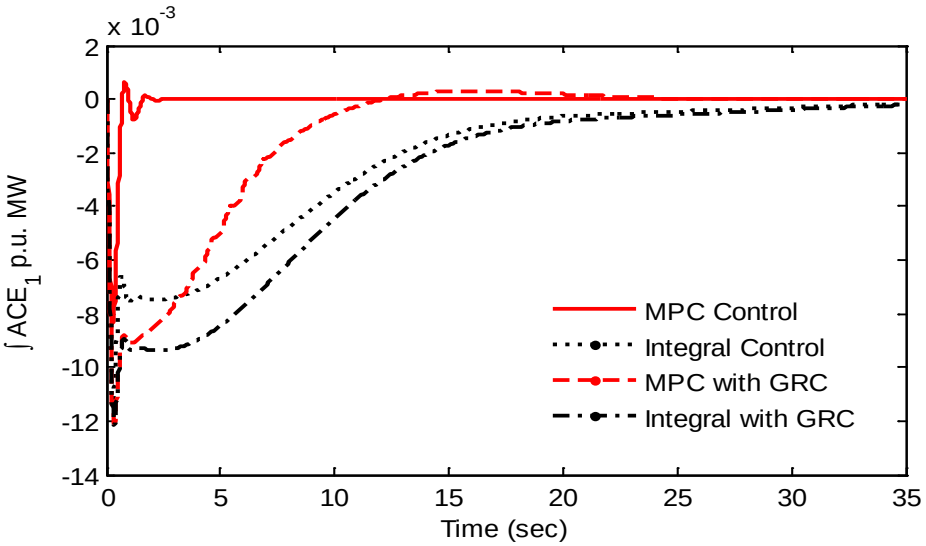

Figure 4.5d: Area control error for 1 % load demand increase with GRC in both areas.

It was observed that by placing the restrictions on power generation in each area, the performance of the MPC deteriorated resulting in a greater overshoot and it took approximately seven seconds longer to reach zero, compared to the MPC without GRC restrictions. However, the MPC still offered acceptable time responses for various system states in comparison to the results achieved with the integral controller. With GRC constraints the system parameters were restored to zero within thirteen seconds with the MPC but the integral controller did not restore the system parameters to zero after thirty-five seconds.

It was necessary to validate the reliability of the MPC performance by varying the power system parameters while the power system experienced a load demand increase. The parameters were varied by ±25 % of their nominal operating values combined with 1 % load increase in area one. In order to check the robust action of the MPC, the following parameters were chosen because they have significant influence on the LFC output:

The time constants of the speed governor (*R*);

The biasing coefficient (*B*) and

Tie-line synchronizing coefficient (T_{12}).

Figures (4.6a -d) show the various system time responses when the system parameters were varied by ±25 % of their nominal operating values while subjected to a 1 % load demand increase in area one.

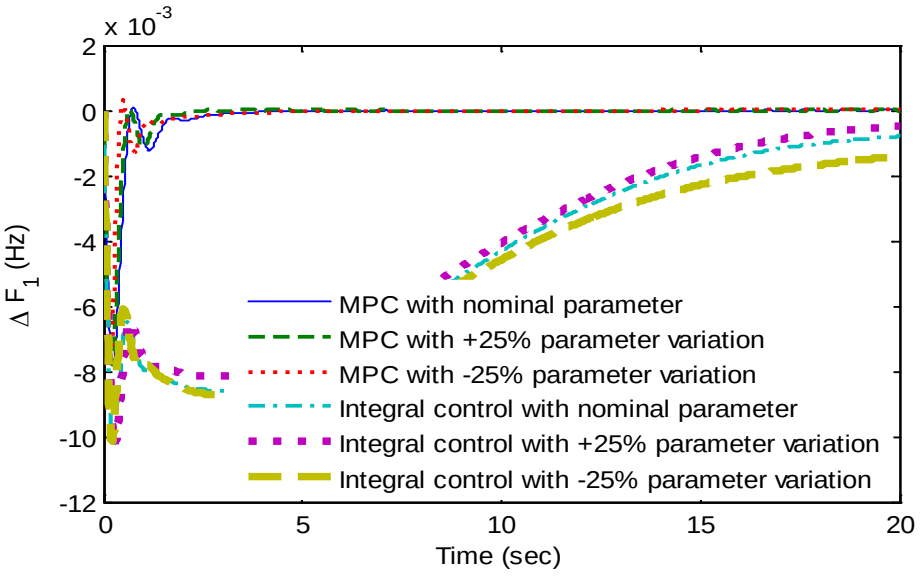

Figure 4.6a: Frequency response in area 1% load increase in area one with 25 % variation in system parameters.

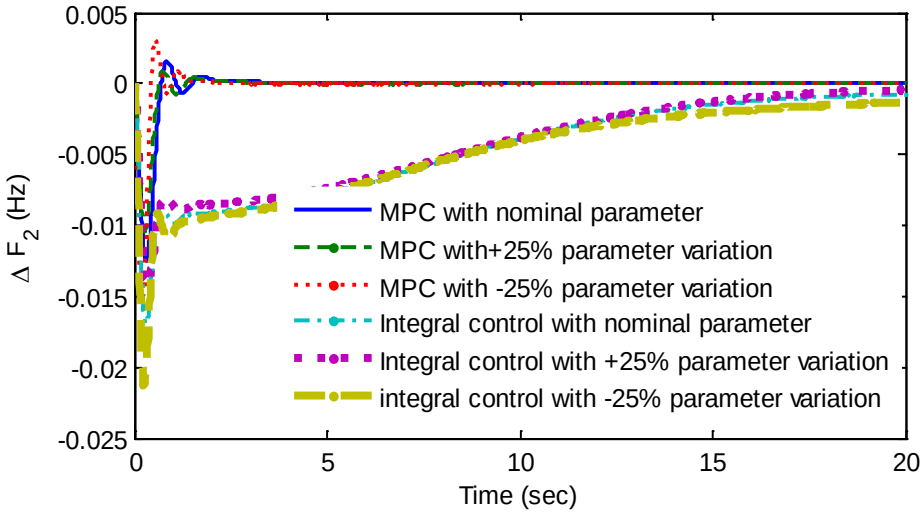

Figure 4.6b: Frequency response in area two for 1% load increase in area one with 25 % variation in system parameters.

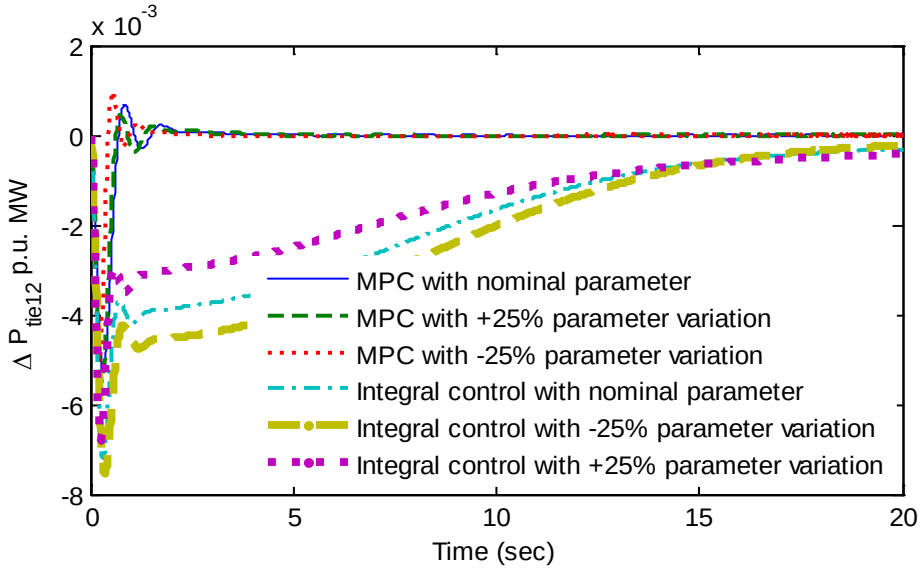

Figure 4.6c: Tie-line power response for 1% load increase in area one with 25 % variation in system parameters.

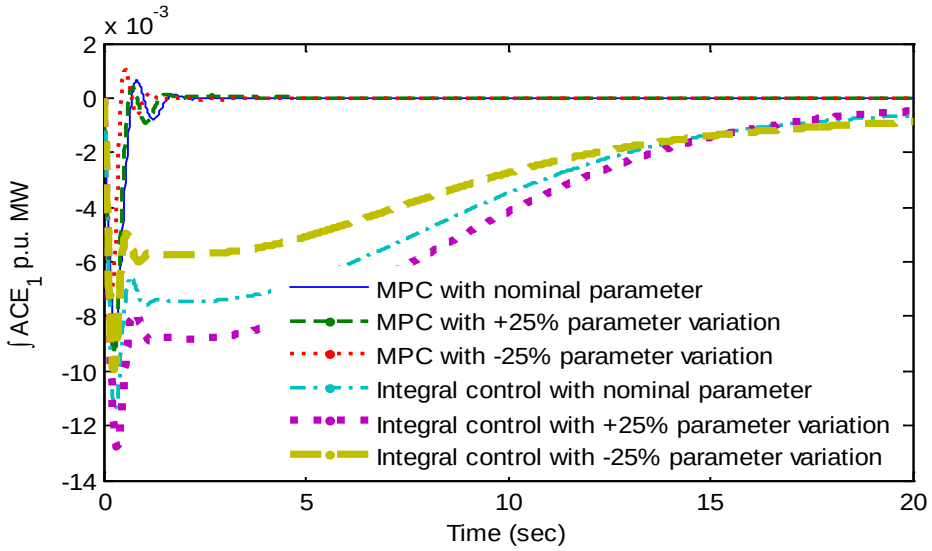

Figure 4.6d: Area control error for 1% load increase in area one with 25 % variation in system parameters.

It was observed that by varying the system parameters, the quality of the LFC deteriorated with the integral controller, which resulted in an increased first peak with a larger settling times. However, no significant change was observed in the performance of the LFC via MPC action.

4.7 Conclusion

This chapter presented the design of a MPC based LFC scheme for a two-area interconnected power system with DFIG in each area in coordination control of TCPS and a SMES unit. The system's dynamic performances were investigated with the proposed MPC based LFC regulator and conventional integral LFC regulator by simulating load fluctuations in one of the power system areas. From the study, it is concluded that the MPC based LFC scheme enhances the system's dynamic performance significantly compared to the results obtained with a conventional integral controller. It was also noted that the MPC scheme is fairly robust and provides a much better dynamic performance even with parameter variations and system non-linearity such as GRC

CHAPTER 5: CONCLUSION

The objective of an electrical power system is to ensure a balance between total power generation and the total load demand, while effectively controlling the power system frequency and tie-line power exchange. This is done in order to provide good quality and reliable power to its consumers. A major concern in power systems is the constantly changing load demands which results in frequency and tie-line power variations which could lead to system instability and possible shutdown of the entire network. Therefore, load frequency control and tie-line power stability are critical control aspects, in interconnected power system design. Hence, this research attempted to investigate an optimal LFC strategy that could be practically implemented.

The design, simulation and analysis of the optimal control strategy for frequency control and tie-line power stability, for sudden load demand fluctuations, were presented in this research work. The control strategy was based on error minimisation through full state vector feedback using the area control error controller. The analysis were done by interpreting the performance index values, eigenvalues, the closed loop feedback gains and the results that were obtained from the simulations. Initially considering 1 % load increase in area one only and later including 2 % load increase in area two, the system's dynamic responses for the three power system models were obtained and analysed. The analysis demonstrated the positive impact of the optimal control strategy in achieving frequency and tie-line power stability for sudden load variations in an interconnected system. The output of the control action was enhanced when the DFIG based wind turbines provided the inertial support in each area, and further improvements were achieved with the combined active power support from a TCPS and a SMES unit. The DFIG based wind turbines in conjunction with the pair of TCPS-SMES improved the capability of the controller in restoring the optimal frequency of the system with lower first peaks, oscillation free system results and faster steady state performances. Although the results in the investigation were positive, optimal control strategies based on full state vector feedback, requires all the state variables to be known. This is virtually impossible

to obtain in a real power system, so numerous assumptions were made during the design process which results in an inaccurate model. Therefore, an alternate control strategy needed to be investigated.

An optimal control strategy based on output feedback, of system parameters that are easily attainable, is a practically alternative to control strategies based on full state vector feedback. Therefore, a load frequency control strategy based on a model predictive control (MPC) concept was investigated. The MPC had a relatively simple design and an inventive control action. It only required two system state parameters; the frequency in each area and the tie-line power variations which were combined to obtain an area control error. The power system model investigated consisted of thermal generations in each area with the active power support from DFIG based wind turbines, combined with the dynamic power support of a TCPS and a SMES unit.

The designed controller was simulated and the system's dynamic responses for various system states were obtained considering a 1% load increase in area one. The robustness of the system was further tested by including GRC restrictions in the simulations. It was also important to validate the MPC performance by varying system parameters. The parameters were varied by ±25 % of their nominal values. The results from the simulations were compared with a conventional integral controller under similar operating conditions. It was observed from the diverse responses that the performance of MPC was far superior compared to the performance of the integral controller. The MPC action was fast enough to match the system load demands with the generated power and provided smoother restoration with lower first peaks of an over shoot. It was also observed that by placing GRC restrictions on the power generation, the performance of the MPC declined, however, the MPC still offered acceptable time responses for various system states in comparison to the results achieved with the integral controller. The analysis revealed that the quality of the LFC, with the integral control, deteriorated significantly with system parameter variations resulting in an

increased first peak with a much longer settling times. However, no significant changes were observed in the performance MPC during parameter variations.

This research tried to present an effective and practical design for LFC and tie-line power stability, for interconnected power systems, incorporating wind generations. The proposed LFC control strategy based on MPC displayed promising results under varying system parameter states and the positive impact of wind power integration using DFIG based wind turbines combined with the active power support of the a TCPS and a SMES unit, were clearly demonstrated. However, there are certain areas which would benefit from further investigations. The scope for future research is presented in the next section.

SCOPE FOR FUTURE RESEARCH

1. The problems of optimal control strategies can be merged with intelligent optimization techniques to obtain better performance index values and improved feedback gains of the controller using optimization techniques.

2. The research can be extended to investigate system nonlinearity's, time delays, random load disturbances and load forecasting, using artificial intelligent techniques to enhance frequency stability studies.

3. The MPC controller can be replaced with a distributed MPC strategy and the research work can be extended to deregulated system environments, considering other renewable energy technologies such as PV combined with the application of other FACTS devices.

REFERENCE

[1] Department of Energy, Republic of South Africa, December 2015.

Available: http://www.energy.gov.za/files/coal_frame.html

[2] Department of Energy, Republic of South Africa, Integrated Resource Plan, 2019.

Available: http://www.energy.gov.za/IRP/irp-2019.html

[3] Department of Minerals and Energy, Republic of South Africa, Integrated Energy Plan for the Republic of South Africa, 19 March 2003.

Available: https://www.gov.za/sites/default/files/gcis_document/201409/dmeintegratedenergyplan190320030.pdf

[4] South African Government, National Development Plan 2030: "Our Future-make it work", 15 August 2012.

Available:https://www.gov.za/documents/national-development-plan-2030-our-future-make-it-work

[5] United Nations General Assembly, "Transforming our world: the 2030 Agenda for Sustainable Development", 25 September 2015.

Available: https://www.un.org/ga/search/view_doc.asp?symbol=A/RES/70/1&Lang=E

[6] Renewable Energy Policy Network for the 21st Century, Renewables 2018: Global Status Report, 5 June 2018.

Available:https://www.ren21.net/wpcontent/uploads/2019/05/GSR2018_Full-Report_English.pdf

[7] Department of Statistics South Africa, Republic of South Africa, "Electricity, gas and water supply industry", 2016

Available:http://www.statssa.gov.za/?page_id=1854&PPN=Report-41-01-02&SCH=7361

[8] Department of Energy, Republic of South Africa, Renewable Energy Independent Power Producer Programme (REIPPP), March 2011.

Available:https://www.iea.org/policies/5393-renewable-energy-independent-power-producer-programme-reippp

[9] Environment, Forestry and Fisheries, Republic of South Africa, “REDZs and Transmission Corridors”.

Available: https://egis.environment.gov.za/redz

[10] CSIR, “Additional renewable energy development zones proposed for wind and solar PV”, November 2019.

Available: https://www.csir.co.za/renewable-energy-development-zones

[11] South African Wind Energy Association, "Cost of wind energy," in Wind Fact Series, ed, 2017.

[12] D. Chetty, G. Sharma and I. Davidson, “Active power regulation of the power system considering DFIG based wind power in coordination with TCPS-SMES,” International Energy Journal, vol. 19, pp. 189–198, 2019.

[13] Ibraheem, P. Kumar and D.P. Kothari, “Recent philosophies of automatic generation control strategies in power systems,” IEEE Transactions on Power Systems vol. 20(1), pp. 346-357, 2005.

[14] A. Demirbas, “Recent advances in biomass conversion technologies” Energy Education Science and Technology, vol. 6, pp. 19-40, 2000.

[15] G. Edwards, “Cost disadvantages of expanding the nuclear power industry,” Canadian Business Review, vol. 9(1), pp19-30, 1982.

[16] World Nuclear Association, “Nuclear power in South Africa,” 2020.

Available:https://www.world-nuclear.org/information-library/country-profiles/countries-o-s/south-africa.aspx

[17] A. Hussain, S.M. Arif and M Aslam, “Emerging renewable and sustainable energy technologies: State of the art,” Renewable and Sustainable Energy Reviews, vol. 71, pp. 12-28, 2017.

[18] Department of Energy, South Africa “South African energy synopsis”, 2010.

Available:http://www.energy.gov.za/files/media/explained/2010/South_African_Energy_Synopsis_2010.pdffckLR

[19] A.F. Zobaa and M. Jovanovic, “A comprehensive overview on reactive power compensation technologies for wind power applications,” International Power Electronics and Motion Control Conference, pp. 1848-1852, 2006.

[20] V. Akhmatov, "Analysis of dynamic behaviour of electric power systems with large amount of wind power," Ph.D, Electrical power engineering, Technical University of Denmark, 2003.

[21] T. Ackermann, “Wind power in power systems”, England: John Wiley and Sons Ltd, 2005.

[22] J. Slootweg, S. De Haan, H. Polinder, and W. Kling, "Modeling wind turbines in power system dynamics simulations," in Power Engineering Society Summer Meeting, IEEE., vol. 1, pp. 22-26, 2001,

[23] J. M. Rodríguez et al., "Incidence on power system dynamics of high penetration of fixed speed and doubly fed wind energy systems: study of the Spanish case," IEEE Transactions on Power Systems, vol. 17, no. 4, pp. 1089-1095, 2002.

[24] A. Khaligh and O.C. Onar, Power Electronics Handbook, Fourth Edition, 2018

[25] Z. Chen and E. Spooner, "Grid power quality with variable speed wind turbines," IEEE Transactions on energy conversion, vol. 16, no. 2, pp. 148-154, 2001.

[26] L. Hansen et al., "Conceptual survey of generators and power electronics for wind turbines," 8755027431, 2002.

[27] M. Dubois, H. Polinder, and J. Ferreira, "Comparison of generator topologies for direct-drive wind turbines," Proceedings of NORPIE'00, pp. 22-26, 2000.

[28] H. El-Helw and S. Tennakoon, "Evaluation of the suitability of a fixed speed wind turbine for large scale wind farms considering the new UK grid code," Renewable Energy, vol. 33, no. 1, pp. 1-12, 2008.

[29] T. Hammons, S. Lee, and K. Low, "Analysis of torques in large steam turbine driven induction generator shafts following disturbances on the system supply," IEEE transactions on energy conversion, vol. 11, no. 4, pp. 693-700, 1996.

[30] F. Jiang, Z. Bo, and L. Roumei, "Performance of induction generator in parallel with an unbalanced three phase system," in International Conference on Power System Technology, 1998, vol. 2, pp. 1193- 1197: IEEE.

[31] S. Salman and B. Badrzadeh, "New Approach for modelling Doubly-Fed Induction Generator (DFIG) for grid-connection studies", European wind energy conference and exhibition, London, vol.1, p. 1, 2004.

[32] Q. Wang and L. Chang, "An intelligent maximum power extraction algorithm for inverter-based variable speed wind turbine systems," IEEE Transactions on power electronics, vol. 19, no. 5, pp. 1242- 1249, 2004.

[33] S. Bhowmik, R. Spee, and J. H. Enslin, "Performance optimization for doubly fed wind power generation systems," IEEE Transactions on Industry Applications, vol. 35, no. 4, pp. 949-958, 1999.

[34] W. Qiao and R. G. Harley, "Effect of grid-connected DFIG wind turbines on power system transient stability," in Power and Energy Society General Meeting-Conversion and Delivery of Electrical Energy in the 21st Century, 2008, pp. 1-7: IEEE.

[35] A. Petersson, "Analysis, modeling and control of doubly-fed induction generators for wind turbines," Chalmers University of Technology, 2005.

[36] J. Muñoz and C. Cañizares, "Comparative stability analysis of DFIG-based wind farms and conventional synchronous generators," in Power Systems Conference and Exposition (PSCE), 2011 IEEE/PES, pp. 1-7: IEEE, 2011.

[37] X. Yingcheng, and T. Nengling, “Review of contribution to frequency control through variable speed wind turbine,” Renew. Energy, vol. 36, no. 6, pp. 1671–1677, 2011.

[38] J. Ekanayake, and N. Jenkins, “Comparison of the response of doubly fed and fixed-speed induction generator wind turbines to change in network frequency,” IEEE Trans. Energy Conversion, vol. 19, no. 4, pp. 800–802, Dec. 2004.

[39] P. Bhatt, R. Roy, and S. P. Ghoshal, “Load frequency control of interconnected restructured power system along with DFIG and coordinated operation of TCPS-SMES,”11th International Conference on Probabilistic Methods Applied to Power Systems (PMAPS 2010), pp. 131–136, Singapore, 14–17 Jun. 2010.

[40] M. Kayikci, and J. V. Milanovic, “Dynamic contribution of DFIG-based wind plants to system frequency disturbances,” IEEE Trans. Power Syst., vol. 24, no. 2, pp. 859–867, May 2009.

[41] J. M. Mauricio, A. Marano, A. Gomez-Exposito, and J. L. M. Ramos, “Frequency regulation contribution through variable-speed wind energy conversion systems,” IEEE Trans. Power Syst., vol. 24, no. 1, pp. 173–180, Feb. 2009.

[42] R. G. De Almeida, and J. A. P. Lopes, “Participation of doubly fed induction wind generators in system frequency regulation,” IEEE Trans. Power Syst., vol. 22, no. 3, pp. 944–950, Aug. 2007.

[43] J. G. Slootweg, S. W. H. de Haan, H. Polinder, and W. L. Kling, “General Model for representing variable speed wind turbines in power system dynamics simulations,” IEEE Trans. Power Syst., vol. 18, no. 1, Feb. 2003.

[44] N. G. Hingorani and L. Gyugyi, “Understanding FACTS,” IEEE press, 2000.

[45] Y. Alharbi, A. S. Yunus, and A. Abu-Siada, "Application of STATCOM to improve the high-voltage-ride-through capability of wind turbine

generator," in Innovative Smart Grid Technologies Asia (ISGT) IEEE PES, pp. 1-5, 2011

[46] T. de Assis, E. H. Watanabe, L. A. S. Pilotto, and R. B. Sollero, "A new technique to control reactive power oscillations using STATCOM," in 10th International Conference on Harmonics and Quality of Power, vol. 2, pp. 607-613: IEEE, 2002.

[47] S. Megh, K. D. Lalit, and N. K. G, "FACTS Devices in Renewable Energy Plants to solve Power System issues," SSRG International Journal of Electrical and Electronics Engineering (SSRG-IJEEE), vol. 3, no. 5, p. 6, 2016.

[48]. J. Chen, S. Song, and Z. Wang, "Analysis and Implement of Thyristor-based STATCOM," in International Conference on Power System Technology, IEEE, pp. 1-5: IEEE, 2006.

[49] X. Zhang, C. Rehtanz, and B. Pal, Flexible AC Transmission Systems: Modelling and Control, Springer-Verlag Berlin Heidelberg, 2006.

[50] I. A. Chidambaram, and B. Paramasivam, “Optimized load-frequency simulation in restructured power system with redox flow batteries and interline power flow controller,” Int. J. Electr. Power Energy Syst.,vol. 50, pp. 9-24, 2013.

[51] H. J. Kunish, K. G. Kramer, and H. Domnik, “Battery energy storage another option for load frequency control and instantaneous reserve,” IEEE Trans. Energy Conv., vol. 1, no. 1, pp. 46-51, 1986.

[52] S. K. Aditya and D. Das, “Battery energy storage for load frequency control of an interconnected power system,” Elect. Power Syst. Res., vol. 58, no. 3, pp. 179-185, Jul. 2001.

[53] P. Breeze, Power System Energy Storage Technologies, Academic Press, 2018.

[54] M. Semadeni, “Storage of energy, overview,” Encyclopedia of Energy, 2004.

[55] L. Wanger, Overview of Energy Storage Technologies, Future Energy,

second edidtion, 2014.

[56] S.C. Tripathy, R. Balasubramanian and P.S.C. Nair, “Adaptive automatic generation control with superconducting magnetic energy storage in power system,” IEEE Trans. Energy Convers., vol. 7, no. 3, pp. 434-441, Sept. 1992.

[57] S.C. Tripathy, R. Balasubramanian and P.S.C. Nair, “Effects of superconducting magnetic energy storage on automatic generation control considering governor dead-band and boiler dynamics,” IEEE Trans. Power Syst., vol. 7, no. 3, pp. 1266-1273, Aug. 1992.

[58] S.C. Tripathy and K.P. Juengst, “Sampled data automatic generation control with superconducting magnetic energy storage in power systems,” IEEE Trans. Energy Convers., vol. 12, no. 2, pp. 187-192, Jun. 1997.

[59] R. J. Abraham, D. Das and A. Patra, “Automatic generation control of an interconnected hydro thermal power system considering superconducting magnetic energy storage,” Int. J. Electr.Power Energy Syst., vol. 29, no. 8, pp. 571-579, 2007.

[60] U.V. Aleem et al., “Static synchronous series compensator (SSSC) as stability booster of a power system,” International Journal of Engineering Trends and Technology, vol. 46, no. 6, April 2017.

[61] B. Balraj, C. Kalaiselvi and G. Selvam, “Design of static synchronous series compensator with CES for interconnected power system,” International Journal of Advances in Engineering and Emerging Technology, Vol. 5, No. 2, April 2014.

[62] H.F. Wang, F.J. Swift and M.Li, “Analysis of thyristor-controlled phase shifter applied in damping power system oscillations,” Electrical Power & Energy Systems, Vol. 19, No. 1, pp. 1-9, 1997.

[63] P. Bhatt, S.P. Ghoshal and R. Roy, “Coordinated control of TCPS and SMES for frequency regulation of interconnected restructured power systems with dynamic participation from DFIG based wind farm,” Renew.

Energy, vol. 40, pp. 40-50, 2012.

[64] P. Bhatt, R. Roy and S.P. Ghoshal, “Comparative performance evaluation of SMES-SMES, TCPS-SMES and SSSC-SMES controllers in automatic generation control for a two area hydrohydro system,” Int. J. Electr. Power Energy Syst., vol. 33, no. 10, pp. 1585-1597, 2011.

[65] P. Bhatt, S. P. Ghoshal and R. Roy, “Load frequency stabilization by coordinated control of thyristor controlled phaseshifters and superconducting magnetic energy storage for three types of interconnected two-area power systems,” Int. J. Electr. Power Energy Syst., vol. 32, no. 10, pp. 1111-1124, 2010.

[66] O.I. Elgerd and C. Fosha. “Optimum megawatt frequency control of multi-area electric energy systems,” IEEE Transactions on Power Apparatus and System, vol. 89(4), pp 556–563, 1970.

[67] H. Bevrani, Robust Power System Control, Springer, New York, pp. 15-61. 2009.

[68] R.C. Bansal and T.S Bhatti, “Small signal analysis of isolated hybrid power systems: reactive power and frequency control analysis,” Alpha Science International, Oxford, U. K. 2008

[69] J.L. Willems, “Sensitivity analysis of the optimum performance of conventional load frequency control,” IEEE Trans. Power Apparat. Syst., vol. 93, no. 5, pp. 1287–1291, Sept. /Oct. 1974.

[70] H.G. Kwatny, and T.A. Athay, “Coordination of economic dispatch and load frequency control in electric power systems,” Proceedings, 18th IEEE Conference on Decision and Control, 1979.

[71] T. Hiyama, “Optimization of discrete-type load-frequency regulators considering generation rate constraints,” Proc. IEE, vol. 129, no. 6, pp. 285–289, Nov. 1982.

[72] M.L. Kothari, P.S. Satsangi, and J. Nanda, “Sampled data automatic control of interconnected reheat thermal stations consisting generation rate constraints,” IEEE Trans. Power Apparat. Syst., vol. 100, no. 5, pp.

2334–2342, May 1981.

[73] M. L. Kothari, P. S. Satsangi, and J. Nanda, “Automatic generation control of an interconnected hydrothermal system in continuous and discrete mode considering generation rate constraints,” Proc. IEE, vol. 130, no.1, pp. 17-27, 1983

[74] M. Jalali, “DFIG based wind turbine contribution to system frequency control”, Ph.D. Thesis, University of Waterloo, Canada, 2011.

[75] K.P.S. Parmar, S. Majhi and D.P. Kothari, “Optimal load frequency control of an interconnected power system,” Int. J. Electr. Instrumentation Engg., vol. 1, no. 1, pp. 1-5, Jan. 2011.

[76] S.J.P.S. Mariano, J.A.N. Pombo, M.R.A. Calado and L.A.F.M. Ferreira, “A procedure to specify the weighting matrices for an optimal load frequency controller,” Turkish Journal of Electrical Engineering and Computer Sciences, vol. 20, no. 2, pp. 1-13, 2012.

[77] A. Kanchanaharuthai, “Optimal sampled-data controller design with time-multiplied performance index for load frequency control,” Proceedings of the IEEE Conference on Control Applications, Taiwan, vol. 1, pp. 655-660 , Sept. 2-4, 2004.

[78] N. Dizdarevic, M. Majstrovic and G Anderson, "FACTS-based reactive power compensation of wind energy conversion system," in IEEE Power Tech Conference Proceedings, Bologna, vol. 2, p. 8 pp. Vol. 2: IEEE, 2003.

[79] G. Sharma, “Optimal AGC design for diverse sources of power generations in each area using output vector feedback control technique,” Int. Journal of Engineering Research in Africa, vol. 45, pp 99-114, 2019.

[80] Ibraheem, K.R. Niazi, G. Sharma, “Study on dynamic participation of wind turbines in AGC of power system,” Electric Power Component and Syst. Vol. 43, pp. 44-55, 2014.

[81] S. Velusami and I. A. Chidambaram, “Decentralized biased dual mode controllers for load frequency control of interconnected power systems considering GDB and GRC non-linearities,” Energy Convers. Manag., vol. 48, no. 5, pp. 1691–1702, 2007.

[82] Z.A. Hanouze, and Y.A. Magid, “Variable structure load frequency controllers for multi area power system,” Int. Journal of Elect. Power & Energy Syst., Vol. 15, pp. 22-29, 1995.

[83] Y.Y. Hsu and W.C. Chan, “Optimal variable structure controller for the load frequency control of interconnected hydrothermal power systems,” Int. J. Electr. Power Energy Syst., vol. 6, no. 4, pp. 221–229, 1984.

[84] G, Sharma G., Ibraheem and K.R. Niazi, “Optimal AGC of asynchronous power systems using output feedback control strategy with dynamic participation of wind turbines,” Electric Power Components and Systems vol. 43(4): pp 384-398, 2015.

[85] T.H.,Mohamed, H. Bevrani, A.A. Hassan and T Hiyama, Decentralized model predictive based load frequency control in an interconnected power system,” Energy Conversion and Management, vol. 52, pp 1208-1214, 2011.

[86] X. Liu, X. Kong, and K.Y. Lee, “Distributed model predictive control for load frequency control with dynamic fuzzy valve position modelling for hydro-thermal power system,” IET Control Theory Appl, vol. 10, no. 14, pp. 1653-1664, 2016.

[87] Y. Zhang, X. Liu, and B, Qu, “Distributed model predictive load frequency control of multi-area power system with DFIGs,” IEEE/CAA Journal of Automatica Sinica, vol. 4, no. 1, pp. 125-135, 2017.

[88] M. Ma, H. Chen, X. Liu, and F. Allgower, “Distributed model predictive load frequency control of multi-area interconnected power system,” Int. J. Electrical Power and Energy Systems, vol. 62, pp. 289-298, 2014.

[89] K.P.S Parmar, S. Majhi, and D.P Kothari, “Load frequency control of a realistic power system with multi-source power generation,” International Journal of Electrical Power and Energy Systems, vol. 42, pp. 426-433. 2012.

Appendix A: Hydro-Thermal Power Plant Data

$P_{r1} = P_{r2} = 2000$ MW

$T_{G1} = 0.08\ s,$

$T_{G2} = 0.2$ s,

$R_1 = R_2 = 2.5$ Hz/p.u.MW, $T_w = 0.1$ s, $T_1 = 0.2$ s, $T_2 = 6$ s,

$T_3 = 0.4$ s,

$K_1 = 0.3,$

$K_2 = 0.4,$

$K_3 = 0.3,$

$b_1 = b_2 = 0.425$ p.u. MW/Hz,

$\Delta P_{d1} = \Delta P_{d2} = 0.01$ p.u. MW,

$K_{p1} = K_{p2} = 120 Hz$(p.u.MW),

$T_{p1} = T_{p2} = 20s.$

Appendix B: Data for DFIG Based Wind Turbines

$H_{e1} = H_{e2} = 3.5\, p.u.\, MW.\, s,$

$T_{w1} = T_{w2} = 6s.$

$K_{\omega p1} = K_{\omega p2} = 1,$

$K_{\omega i1} = K_{\omega i2} = 0.5,\ T_{a1} = T_{a2} = 0.2s,\ T_{r1} = T_{r2} = 15s,$

Appendix C: Thermal-Thermal Power Plant Data

Area-1	Area-2	Description	Value
H_{e1}	H_{e2}	Wind turbine inertia	3.5 p.u. MW.s
K_{p1}	K_{p2}	Power system gain	120 Hz/(p.u. MW)
K_{wp1}	K_{wp2}	DFIG proportional controller gain	2
K_{wi1}	K_{wi2}	DFIG integral controller gain	0.5
T_{12}	-	Tie-line synchronizing coefficient	0.545 p.u. MW/Hz
T_{h1}	T_{h2}	Governor time constant	0.08 s
T_{t1}	T_{t2}	Turbine time constant	0.3 s
T_{p1}	T_{p2}	Power system time constant	20 s
T_{a1}	T_{a2}	DFIG turbine	0.2 s
T_{r1}	T_{r2}	Transducer time constant	15 s
T_{w1}	T_{w2}	Washout filter time constant	6 s
R_1	R_2	Regulation droop	2.4Hz/(p.u. MW)
B_1	B_2	Biasing coefficient	0.425p.u.MW/Hz
-	L	Inductance of coil	2.65 H
-	T_{DC}	Converter time delay	0.03 s
-	K_{SMES}	Gain of control loop	100 kV/unit MW
-	K_{id}	Gain for feedback	0.2 kV/kA

Appendix D: Optimal Control System Matrices

State matrix $[A_2]$ =

$$\begin{bmatrix}
0 & 0 & 0 & B_1 & 1 & 0 & 0 & 0 & 0 & 0 & 0 & 0 & 0 & 0 & 0 & 0 & 0 & 0 & 0 & 0 & 0 & 1 \\
0 & \frac{-1}{T_{G1}} & 0 & \frac{-1}{R_1 T_{G1}} & 0 & 0 & 0 & 0 & 0 & 0 & 0 & 0 & 0 & 0 & 0 & 0 & 0 & 0 & 0 & 0 & 0 & 0 \\
0 & \frac{T_{G1}+T_W}{0.5T_{G1}T_W} & \frac{-1}{0.5T_W} & \frac{1}{0.5R_1T_{G1}} & 0 & 0 & 0 & 0 & 0 & 0 & 0 & 0 & 0 & 0 & 0 & 0 & 0 & 0 & 0 & 0 & 0 & 0 \\
0 & 0 & \frac{K_{P1}}{T_{P1}} & \frac{-1}{T_{P1}} & \frac{-K_{P1}}{T_{P1}} & 0 & 0 & 0 & \frac{K_{P1}}{T_{P1}} & 0 & 0 & 0 & 0 & 0 & 0 & 0 & 0 & 0 & 0 & 0 & 0 & \frac{-K_{P1}}{T_{P1}} \\
0 & 0 & 0 & 2\pi T & 0 & 0 & 0 & 0 & 0 & 0 & 0 & 0 & 0 & 0 & 0 & -2\pi T & 0 & 0 & 0 & 0 & 0 & 0 \\
0 & 0 & 0 & \frac{1}{T_{r1}} & 0 & \frac{-1}{T_{r1}} & 0 & 0 & 0 & 0 & 0 & 0 & 0 & 0 & 0 & 0 & 0 & 0 & 0 & 0 & 0 & 0 \\
0 & 0 & 0 & \frac{1}{T_{r1}} & 0 & \frac{-1}{T_{r1}} & \frac{-1}{T_{w1}} & 0 & 0 & 0 & 0 & 0 & 0 & 0 & 0 & 0 & 0 & 0 & 0 & 0 & 0 & 0 \\
0 & 0 & 0 & 0 & 0 & 0 & 0 & -K_{wi1} & 0 & 0 & 0 & 0 & 0 & 0 & 0 & 0 & 0 & 0 & 0 & 0 & 0 & 0 \\
0 & 0 & 0 & 0 & 0 & 0 & \frac{-1}{R_1 T_{a1}} & \frac{-1}{T_{a1}} & \frac{-1}{T_{a1}} & \frac{-K_{wp1}}{T_{a1}} & 0 & 0 & 0 & 0 & 0 & 0 & 0 & 0 & 0 & 0 & 0 & 0 \\
0 & 0 & 0 & 0 & 0 & 0 & 0 & 0 & \frac{1}{2H_{e1}} & 0 & 0 & 0 & 0 & 0 & 0 & 0 & 0 & 0 & 0 & 0 & 0 & 0 \\
0 & 0 & 0 & 0 & a_{12} & 0 & 0 & 0 & 0 & 0 & 0 & 0 & 0 & 0 & 0 & B_2 & 0 & 0 & 0 & 0 & 0 & a_{12} \\
0 & 0 & 0 & 0 & 0 & 0 & 0 & 0 & 0 & 0 & 0 & \frac{-1}{T_{G2}} & 0 & 0 & 0 & \frac{-1}{R_2 T_{G2}} & 0 & 0 & 0 & 0 & 0 & 0 \\
0 & 0 & 0 & 0 & 0 & 0 & 0 & 0 & 0 & 0 & 0 & \frac{1}{T_1} & \frac{-1}{T_1} & 0 & 0 & 0 & 0 & 0 & 0 & 0 & 0 & 0 \\
0 & 0 & 0 & 0 & 0 & 0 & 0 & 0 & 0 & 0 & 0 & 0 & \frac{1}{T_2} & \frac{-1}{T_2} & 0 & 0 & 0 & 0 & 0 & 0 & 0 & 0 \\
0 & 0 & 0 & 0 & 0 & 0 & 0 & 0 & 0 & 0 & 0 & \frac{K_1}{T_1} & \frac{K_1}{T_3}-\frac{K_1}{T_1}+\frac{K_2}{T_2} & \frac{K_2}{T_3}+\frac{K_3}{T_3}-\frac{K_2}{T_2} & \frac{-1}{T_3} & 0 & 0 & 0 & 0 & 0 & 0 & 0 \\
0 & 0 & 0 & 0 & \frac{a_{12}K_{P2}}{T_{P2}} & 0 & 0 & 0 & 0 & 0 & 0 & 0 & 0 & 0 & \frac{K_{P2}}{T_{P2}} & \frac{-1}{T_{P2}} & 0 & 0 & 0 & \frac{K_{P2}}{T_{P2}} & 0 & \frac{K_{P2}}{T_{P2}} \\
0 & 0 & 0 & 0 & 0 & 0 & 0 & 0 & 0 & 0 & 0 & 0 & 0 & 0 & 0 & \frac{1}{T_{r2}} & \frac{-1}{T_{r2}} & 0 & 0 & 0 & 0 & 0 \\
0 & 0 & 0 & 0 & 0 & 0 & 0 & 0 & 0 & 0 & 0 & 0 & 0 & 0 & 0 & \frac{1}{T_{r2}} & \frac{-1}{T_{r2}} & \frac{-1}{T_{w2}} & 0 & 0 & 0 & 0 \\
0 & 0 & 0 & 0 & 0 & 0 & 0 & 0 & 0 & 0 & 0 & 0 & 0 & 0 & 0 & 0 & 0 & 0 & -K_{wi2} & 0 & 0 & 0 \\
0 & 0 & 0 & 0 & 0 & 0 & 0 & 0 & 0 & 0 & 0 & 0 & 0 & 0 & 0 & 0 & 0 & \frac{-1}{R_2 T_{a2}} & \frac{-1}{T_{a2}} & \frac{-1}{T_{a2}} & \frac{-K_{wp2}}{T_{a2}} & 0 \\
0 & 0 & 0 & 0 & 0 & 0 & 0 & 0 & 0 & 0 & 0 & 0 & 0 & 0 & 0 & 0 & 0 & 0 & 0 & \frac{1}{2H_{e2}} & 0 & 0 \\
0 & 0 & 0 & \frac{K_{dc}}{T_{dc}} & 0 & 0 & 0 & 0 & 0 & 0 & 0 & 0 & 0 & 0 & 0 & \frac{-K_{dc}}{T_{dc}} & 0 & 0 & 0 & 0 & 0 & \frac{-1}{T_{dc}}
\end{bmatrix}.$$

Control matrix:

$$[B_2]^T = \begin{bmatrix}
0 & \frac{1}{T_{G1}} & \frac{-1}{0.5T_{G1}} & 0 & 0 & 0 & 0 & 0 & 0 & \frac{-1}{2H_{e1}} & 0 & 0 & 0 & 0 & 0 & 0 & 0 & 0 & 0 & 0 & 0 \\
0 & 0 & 0 & 0 & 0 & 0 & 0 & 0 & 0 & 0 & 0 & \frac{1}{T_{G2}} & 0 & 0 & 0 & 0 & 0 & 0 & 0 & \frac{-1}{2H_{e2}} & 0
\end{bmatrix}.$$

Disturbance matrix:

$$[\Gamma_2]^T = \begin{bmatrix}
0 & 0 & 0 & \frac{-K_{P1}}{T_{P1}} & 0 & 0 & 0 & 0 & 0 & 0 & 0 & 0 & 0 & 0 & 0 & 0 & 0 & 0 & 0 & 0 & 0 & 0 \\
0 & 0 & 0 & 0 & 0 & 0 & 0 & 0 & 0 & 0 & 0 & 0 & 0 & 0 & 0 & \frac{-K_{P2}}{T_{P2}} & 0 & 0 & 0 & 0 & 0 & 0
\end{bmatrix}.$$